

A Survey on Vision Mamba: Models, Applications and Challenges

Rui Xu, Shu Yang, Yihui Wang, Bo Du, *Senior Member, IEEE*, Hao Chen, *Senior Member, IEEE*

Abstract—Mamba, a recent selective structured state space model, performs excellently on long sequence modeling tasks. Mamba mitigates the modeling constraints of convolutional neural networks and offers advanced modeling capabilities similar to those of Transformers, through global receptive fields and dynamic weighting. Crucially, it achieves this without incurring the quadratic computational complexity typically associated with Transformers. Due to its advantages over the former two mainstream foundation models, Mamba exhibits great potential to be a visual foundation model. Researchers are actively applying Mamba to various computer vision tasks, leading to numerous emerging works. To help keep pace with the rapid advancements in computer vision, this paper aims to provide a comprehensive review of visual Mamba approaches. This paper begins by delineating the formulation of the original Mamba model. Subsequently, our review of visual Mamba delves into several representative backbone networks to elucidate the core insights of the visual Mamba. We then categorize related works using different modalities, including image, video, point cloud, multi-modal, and others. Specifically, for image applications, we further organize them into distinct tasks to facilitate a more structured discussion. Finally, we discuss the challenges and future research directions for visual Mamba, providing insights for future research in this quickly evolving area. A comprehensive list of visual Mamba models reviewed in this work is available at <https://github.com/Ruixxxx/Awesome-Vision-Mamba-Models>.

Index Terms—Mamba, State Space Model, Computer Vision.

I. INTRODUCTION

ARTIFICIAL intelligence technologies, especially deep learning, have revolutionized numerous application fields. In the field of computer vision (CV), convolutional neural networks (CNNs) utilize convolutional layers to process visual data, capitalizing on inductive biases such as locality and spatial invariance [1]–[3]. Despite their linear computational complexity and versatile modeling ability, CNNs have restricted receptive fields. In recent years, Vision Transformers (ViTs) [4], which utilize a self-attention mechanism [5] to process sequences of image patches, have demonstrated remarkable modeling capabilities across various visual tasks [6].

Corresponding author: *Hao Chen*.

Rui Xu, Shu Yang and Yihui Wang are with the Department of Computer Science and Engineering, The Hong Kong University of Science and Technology, Hong Kong, China (e-mail: rui.xu@whu.edu.cn, {syangcw, ywangrm}@connect.ust.hk).

Bo Du is with the School of Computer Science, National Engineering Research Center for Multimedia Software, Institute of Artificial Intelligence and Hubei Key Laboratory of Multimedia and Network Communication Engineering, Wuhan University, Wuhan 430072, China (e-mail: dubo@whu.edu.cn).

Hao Chen is with the Department of Computer Science and Engineering, the Department of Chemical and Biological Engineering and the Division of Life Science, The Hong Kong University of Science and Technology, Hong Kong, China (e-mail: jhc@cse.ust.hk).

However, the self-attention mechanism involves a quadratic computational cost to the number of patches, which limits the scalability of ViTs. The CV domain has long been dominated by CNNs and ViTs, each with their respective strengths and inherent limitations. To overcome their limitations, researchers have devoted significant effort to improving these models. Recently, structured state space models [7], [8] have garnered considerable attention due to their computational efficiency and principled capability in modeling long-range dependencies [9].

The state space model is a concept that is widely adopted in various disciplines. Its core idea is connecting the input and output sequences using a latent state. It takes different forms in different disciplines, such as Markov decision process in reinforcement learning [10], dynamic causal modeling in computational neuroscience [11] and Kalman filters in controls [12]. Recently, the state space model (SSM) has been introduced to deep learning for sequence modeling and its parameters or mappings are learned by gradient descent [13]. SSM is essentially a type of sequence transformation and can be incorporated into deep neural networks. It conceptually unifies the strengths of former sequence models including continuous-time models (CTMs), recurrent neural networks (RNNs), and CNNs. However, SSMs have not been widely used in practice due to their extensive computational and memory requirements coming from the state representation. This situation has changed with the advent of the structured SSM (S4), which addresses these limitations through reparameterizing the state matrices A [7]. Since then, a series of SSMs and SSM architectures emerge [7], [8], [14]–[18]. However, SSMs' constant sequence transitions restrict their context-based reasoning ability, which is important for the efficacy of models like Transformer [5]. In [19], the authors propose to address this by integrating a selection mechanism into the SSM, thus enabling the SSM to selectively propagate or forget information along the sequence or scan path based on the current token. Subsequently, the authors integrate these selective SSMs into a simplified neural network architecture, termed as Mamba. With the modeling power akin to Transformers and linear scalability in sequence length, Mamba becomes a promising foundation model for sequence modeling tasks.

Given the frequent cross-pollination between CV and sequence modeling or natural language processing (NLP) approaches, there is a rapid application of Mamba [19] to CV tasks. VMamba [20] is an early representative visual Mamba model. It unfolds image patches into sequences along the horizontal and vertical dimensions of the image, and performs bi-directional scanning along these two directions. Another

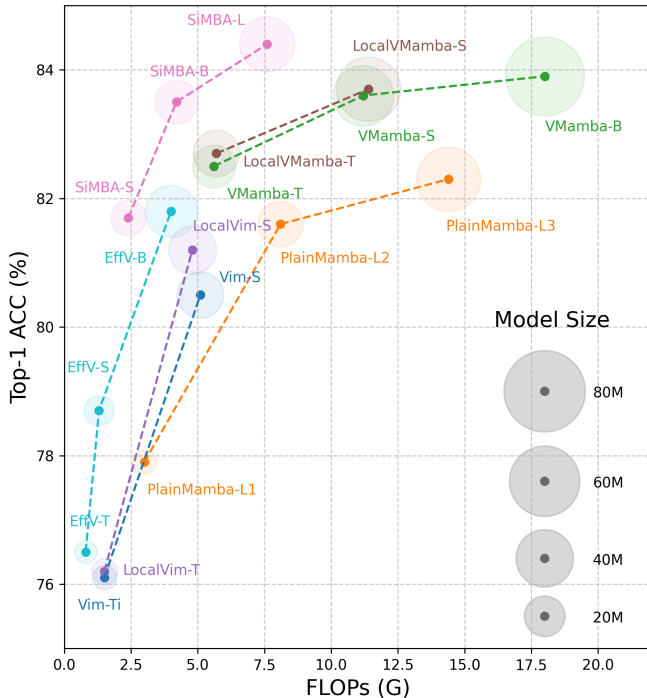


Fig. 1: Comparison of performance and computational complexity for representative visual Mamba backbone networks. The diameter of each circle is proportional to the respective model’s parameter count, providing a visual cue for the model’s complexity.

visual Mamba model Vim [21] leverages position embeddings to incorporate spatial information, inspired by ViT [4]. It also uses bi-directional SSM for handling the non-causal image sequences. Similarly, several other notable studies [22]–[26] delve into the exploration of visual backbone networks, consistently achieving competitive performance across classification, detection, and segmentation tasks. To highlight the balance between efficiency and effectiveness in visual Mamba models, Fig. 1 offers a graphical representation contrasting their performance with computational complexity, where the relative size of each model is indicated visually. In addition to these efforts, Mamba has been applied across a diverse range of vision modalities and their respective applications, encompassing image processing, video analysis, point cloud processing, multi-modal scenarios, and more. Endowed with the aforementioned modeling capability and linear scalability, Mamba stands out as a promising foundation model for CV tasks. The growing interest among researchers in applying Mamba to various vision tasks is reflected in the increasing number of studies dedicated to this exploration.

In the rapidly evolving field of CV, Mamba [19] has emerged as a significant advancement. Keeping pace with the latest research is critical for the community. Therefore, this paper aims to provide a comprehensive review of the applications of Mamba in visual tasks, shedding light on both its foundational elements and diverse applications across various modalities. Our contributions are summarized as follows:

1. **Formulation of Mamba** (Section II): We provide an introductory overview of the operational principles of the Mamba [19] and state space models.
2. **Backbone Networks** (Section III): We provide a detailed examination of several representative visual Mamba backbone networks. This analysis aims to elucidate the core principles and innovations that underpin the Visual Mamba framework.
3. **Applications** (Section IV): We categorize other applications of Mamba by different modalities, such as image, video, point cloud, multi-modal data, and others. Each category is explored in depth to highlight how the Mamba framework adapts to and benefits each modality. For applications involving images, we further divide them into various tasks including but not limited to classification, detection, and segmentation.
4. **Challenges** (Section V): We examine the challenges associated with CV by analyzing the unique characteristics of visual data, the underlying mechanisms of algorithms, and the practical concerns of real-world applications.
5. **Future Directions** (Section VI): We explore prospective research directions in visual Mamba, focusing on potential advancements in data utilization and algorithmic development.

II. FORMULATION OF MAMBA

Mamba [19] is a recent sequence model aiming at improving the context-based reasoning ability of SSM by simply making its parameters to be functions of the input. The SSM here especially refers to the sequence transformation used in the structured state space sequence model (S4) [7], which can be incorporated into deep neural networks. Mamba simplifies the commonly used SSM block and forms a simplified SSM architecture. In the following, we elaborate on the core concepts of Mamba.

A. SSM

The SSM transformation in S4 [7] originates from the classical state space model, which maps a 1D input signal $x(t) \in \mathbb{R}$ to a 1D output signal $y(t) \in \mathbb{R}$ through an N-D latent state $h(t) \in \mathbb{R}^N$:

$$\begin{aligned} h'(t) &= \mathbf{A}h(t) + \mathbf{B}x(t), \\ y(t) &= \mathbf{C}h(t), \end{aligned} \quad (1)$$

where $\mathbf{A} \in \mathbb{R}^{N \times N}$, $\mathbf{B} \in \mathbb{R}^{N \times 1}$, $\mathbf{C} \in \mathbb{R}^{1 \times N}$ are parameters of neural networks in deep learning. To deal with the discrete input sequence $\mathbf{x} = (x_0, x_1, \dots) \in \mathbb{R}^L$, following previous work [27], S4 discretizes these parameters in Eq. (1) using a step size Δ , which can be seen as the resolution of the continuous input $x(t)$. In particular, the continuous parameters \mathbf{A}, \mathbf{B} are converted into discrete parameters $\bar{\mathbf{A}}, \bar{\mathbf{B}}$ by the zero-order hold (ZOH) defined as:

$$\begin{aligned} \bar{\mathbf{A}} &= \exp(\Delta\mathbf{A}), \\ \bar{\mathbf{B}} &= (\Delta\mathbf{A})^{-1}(\exp(\Delta\mathbf{A}) - \mathbf{I}) \cdot \Delta\mathbf{B}. \end{aligned} \quad (2)$$

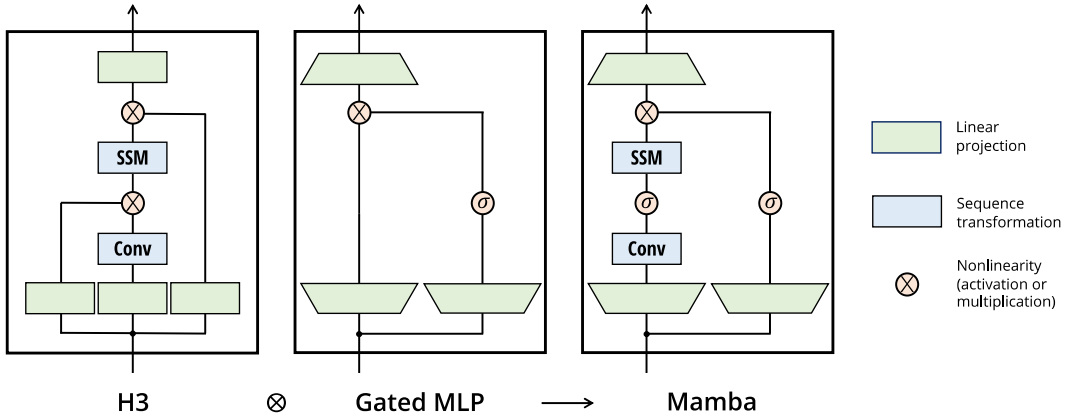


Fig. 2: Mamba block, a simplified block that integrates the H3 and MLP blocks (image from [19]).

After discretizing \mathbf{A}, \mathbf{B} to $\bar{\mathbf{A}}, \bar{\mathbf{B}}$, the Eq. (1) can be reformulated as:

$$\begin{aligned} h_t &= \bar{\mathbf{A}}h_{t-1} + \bar{\mathbf{B}}x_t, \\ y_t &= \mathbf{C}h_t. \end{aligned} \quad (3)$$

Then SSM can be efficiently computed by RNN. This recursive process can also be reformulated and computed as a convolution:

$$\begin{aligned} \bar{\mathbf{K}} &= (\mathbf{C}\bar{\mathbf{B}}, \mathbf{C}\bar{\mathbf{A}}\bar{\mathbf{B}}, \dots, \mathbf{C}\bar{\mathbf{A}}^{L-1}\bar{\mathbf{B}}), \\ \mathbf{y} &= \mathbf{x} * \bar{\mathbf{K}}, \end{aligned} \quad (4)$$

where L denotes the length of the input sequence \mathbf{x} and $\bar{\mathbf{K}} \in \mathbb{R}^L$ is the SSM convolution kernel.

B. Selective SSM

As seen, the parameters in SSM indicated by either Eq. (1), Eq. (3) or Eq. (4) remain invariant with respect to the input or temporal dynamics. Mamba [19] identifies this linear time-invariant (LTI) property as a fundamental limitation of SSM when it comes to context-based reasoning. To address this issue, Mamba incorporates a selection mechanism. The selection mechanism is implemented by simply making the parameters of SSM functions of the input, thus achieving input-dependent interactions along the sequence. Specifically, parameters $\mathbf{B}, \mathbf{C}, \Delta$ are dependent on the input sequence \mathbf{x} :

$$\mathbf{B}, \mathbf{C}, \Delta = \text{Linear}(\mathbf{x}), \quad (5)$$

where $\mathbf{B} \in \mathbb{R}^{B \times L \times N}$, $\mathbf{C} \in \mathbb{R}^{B \times L \times N}$, and $\Delta \in \mathbb{R}^{B \times L \times D}$. Here we present the complete shape of $\mathbf{x} \in \mathbb{R}^{B \times L \times D}$, where B denotes batch size and D is the number of channels. The authors in [19] employ hardware-aware techniques to efficiently compute the selective SSM.

C. Mamba Architecture

Mamba is a simplified SSM architecture. Unlike the commonly used SSM architectures, which stack the linear attention-like block and multi-layer perceptron (MLP) block as Transformers, Mamba integrates these two fundamental blocks to construct the Mamba block. As illustrated in Fig. 2, the Mamba block can be viewed from two distinct perspectives. Firstly, it replaces the multiplicative gate in the linear

attention-like or H3 [28] block with an activation function. Secondly, it incorporates the SSM transformation into the primary pathway of the MLP block. The overall architecture of Mamba consists of repeated Mamba blocks interleaved with standard normalization layers and residual connections.

Mamba inherits the linear scalability in sequence length of the state space models, and also realizes the modeling ability of Transformers. Mamba combines the significant advantages of two primary types of foundation models in CV, i.e. CNNs and Transformers, making it a promising foundation model for CV. In contrast to Transformers, which rely on explicitly storing the entire context for context-based reasoning, Mamba utilizes a selection mechanism. Thus the 1D and causal characteristics of this selection mechanism become focal points for researchers applying Mamba to CV.

III. BACKBONE FOR REPRESENTATION LEARNING

In this section, we review several representative visual Mamba backbone networks to clarify the fundamental principles and innovations of applying Mamba to CV.

A. Pure Mamba

1) *Vim*: Vim [21] is a Mamba-based architecture directly operating on image patch sequences similar to ViT. The input image is first transformed into flattened 2D patches, which are then vectorized using a linear projection layer and added with position embeddings to retain spatial information. Following ViT [4] and BERT [41], a class token is appended to the sequences of patch tokens. The overall token sequence is then fed into the Vim encoder, which consists of identical Vim blocks. As illustrated in Fig. 3 (b), the Vim block is a Mamba block integrating a backward SSM path alongside the forward one.

2) *VMamba*: VMamba [20] identifies two challenges in applying Mamba to 2D images, which are induced by the 1D and causal attributes of the selection mechanism in Mamba. Causally processing the input data makes Mamba unable to assimilate information from the portion of the unscanned data. Moreover, 1D scanning is not optimal for images involving 2D spatial information pertinent on both local and global scales.

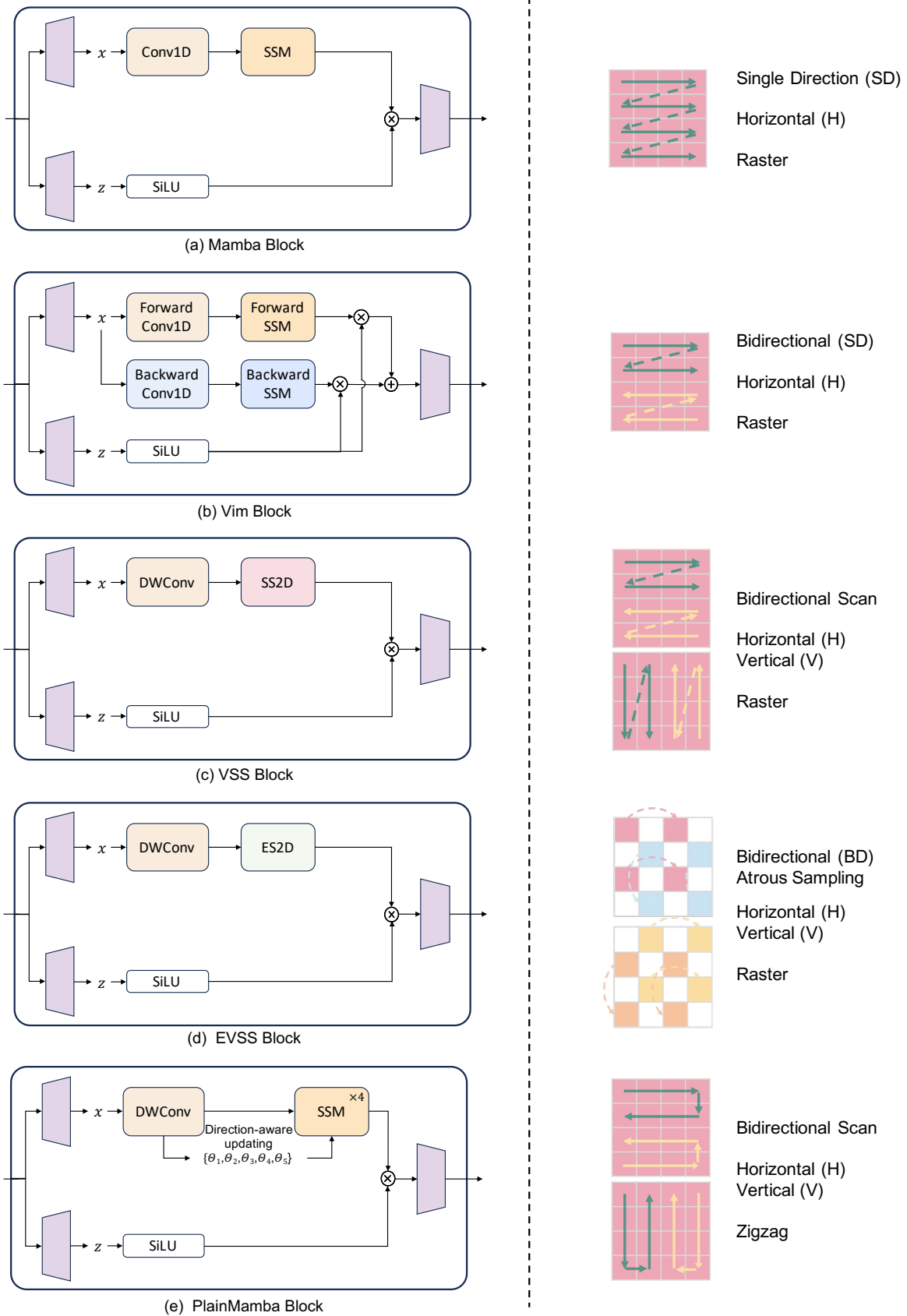


Fig. 3: Visual Mamba blocks, including Vim Block, VSS Block, EVSS Block, and PlainMamba Block. The original Mamba Block is presented as a reference for the advancements in the visual Mamba blocks.

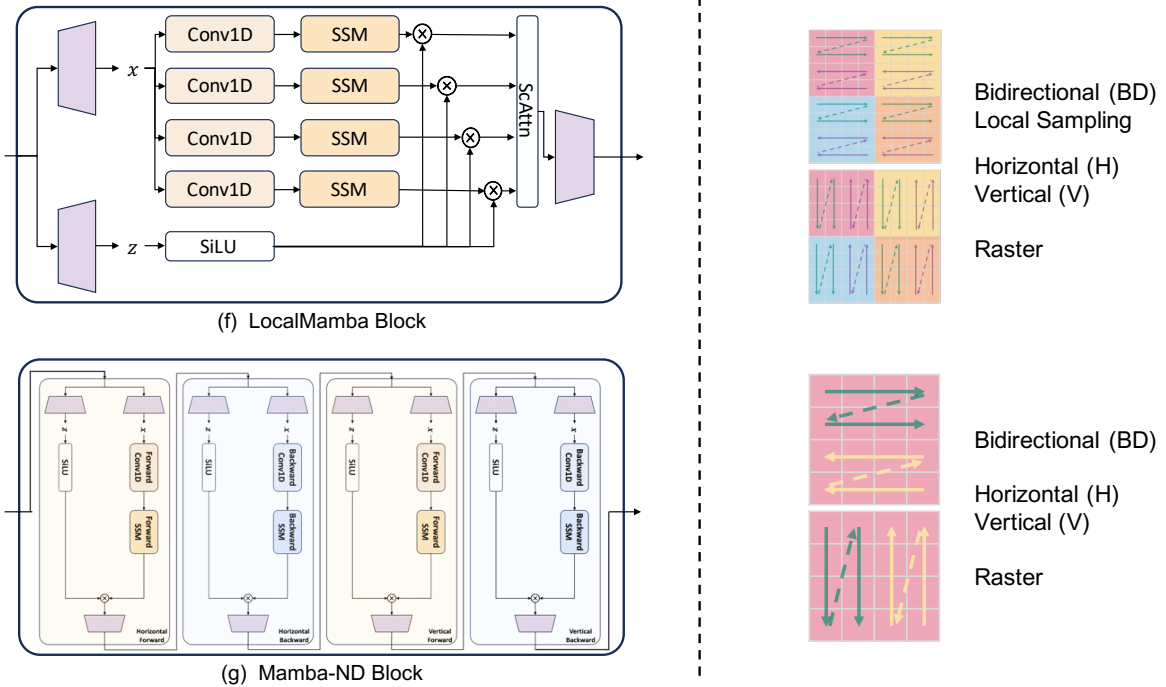


Fig. 4: Visual Mamba blocks, including LocalMamba Block and Mamba-ND Block.

To address the two challenges, VMamba introduces a Cross-Scan Module (CSM) using bidirectional scan mode and horizontal and vertical scan axes as depicted in Fig. 3 (c). The CSM transforms the input image into sequences of patches along both horizontal and vertical axes (*scan expand*), to scan the sequences in four directions: from the top-left to the bottom-right, the bottom-right to the top-left, the top-right to the bottom-left, and the bottom-left to the top-right. Then the resulting four sequences are individually processed using selective SSMs. This operation can also be seen as performing bi-directional selective SSMs along 2D axes. Consequently, each pixel integrates information from all other pixels in four different directions. Finally, all sequences are transformed into their original 2D layout to constitute images and merged to obtain a new image (*scan merge*). The whole process of *scan expand*, selective SSM, and *scan merge* constitutes the 2D-Selective-Scan (SS2D).

VMamba first transforms the input image into 2D patches. Then they are fed into multiple stages of VMamba, which are comprised of stacked Visual State Space (VSS) blocks, and down-sampling operations [42] are inserted between these stages to construct the overall hierarchical architecture. VMamba introduces two kinds of VSS blocks, the vanilla VSS block as shown in Fig. 3 (c) and VSS block. The vanilla VSS block is similar to the Mamba block but replaces the 1D convolution layer with a 2D depth-wise convolution layer and the selective SSM with SS2D plus a layer normalization (LN) layer. The VSS block resembles the typical Transformer blocks.

3) *Mamba-ND*: Mamba-ND [22] aims to extend Mamba to multi-dimensional data including images and videos. It treats 1D Mamba layer as a black box and explores how to unravel

and order the multi-dimensional data. It mainly addresses the challenges presented by data lacking a predefined ordering while possessing inherent spatial dimensions. Given the large quantities of possible ways of flattening the data into 1D sequence, Mamba-ND only includes the scan ordering by flattening the data along its dimension axes in the forward or backward direction. Then it applies the Mamba-ND block, which is a combination of 1D Mamba layers, to the sequence in alternating orderings. The authors conduct extensive experiments to explore different combinations of orderings. In addition, they split the input data’s one dimension into the number of orderings, adopt different arrangements of Mamba layers, and factorize the sequence into smaller sequences. Results show that a chain of Mamba layers and simple alternating-directional orderings achieve superior performance. The final design of the Mamba-ND block is as depicted in Fig. 4 (g).

4) *PlainMamba*: PlainMamba [23] is crafted as a non-hierarchical architecture to fulfill several objectives: (1) a non-hierarchical structure facilitates multi-level feature fusion, enhancing integration across different scales; (2) it supports effective fusion of multi-modal data; (3) its simpler architecture tends to offer better generalization capabilities; (4) it is amenable to optimization for hardware acceleration.

Initially, the input image is transformed into 2D patch tokens, and combined with position embeddings to preserve spatial information. Unlike ViT [4], no special token, such as the class token, is used. Then these tokens are processed by a series of identical PlainMamba blocks, as shown in Fig. 3 (e). The PlainMamba block is similar to the Mamba block, except that the 2D depth-wise convolution layer is employed to substitute the 1D convolution layer, and more importantly,

TABLE I: Comparison of different backbones on ImageNet-1K classification.

Backbone	Image Size	Params	FLOPs	Top-1 ACC
ConvNets				
RegNetY-4G [29]	224 ²	21M	4.0G	80.0
RegNetY-8G [29]	224 ²	39M	8.0G	81.7
RegNetY-16G [29]	224 ²	84M	16.0G	82.9
EffNet-B3 [30]	300 ²	12M	1.8G	81.6
EffNet-B4 [30]	380 ²	19M	4.2G	82.9
EffNet-B5 [30]	456 ²	30M	9.9G	83.6
EffNet-B6 [30]	528 ²	43M	19.0G	84.0
Transformers				
ViT-B/16 [4]	384 ²	86M	55.4G	77.9
ViT-L/16 [4]	384 ²	307M	190.7G	76.5
DeiT-Ti [31]	224 ²	6M	1.3G	72.2
DeiT-S [31]	224 ²	22M	4.6G	79.8
DeiT-B [31]	224 ²	86M	17.5G	81.8
DeiT-B [31]	384 ²	86M	55.4G	83.1
Swin-T [6]	224 ²	29M	4.5G	81.3
Swin-S [6]	224 ²	50M	8.7G	83.0
Swin-B [6]	224 ²	88M	15.4G	83.5
SSMs				
S4ND-ViT-B [32]	224 ²	89M	-	80.4
S4ND-ConvNeXt-T [32]	224 ²	30M	-	82.2
Vim-Ti [21]	224 ²	7M	1.5G	76.1
Vim-S [21]	224 ²	26M	5.1G	80.5
PlainMamba-L1 [23]	224 ²	7M	3.0G	77.9
PlainMamba-L2 [23]	224 ²	25M	8.1G	81.6
PlainMamba-L3 [23]	224 ²	50M	14.4G	82.3
Mamba-2D-S [22]	224 ²	24M	-	81.7
Mamba-2D-B [22]	224 ²	92M	-	83.0
VMamba-T [20]	224 ²	22M	5.6G	82.5
VMamba-S [20]	224 ²	44M	11.2G	83.6
VMamba-B [20]	224 ²	75M	18G	83.9
EffVMamba-T [26]	224 ²	6M	0.8G	76.5
EffVMamba-S [26]	224 ²	11M	1.3G	78.7
EffVMamba-B [26]	224 ²	33M	4.0G	81.8
LocalVim-T [25]	224 ²	8M	1.5G	76.2
LocalVim-S [25]	224 ²	28M	4.8G	81.2
LocalVMamba-T [25]	224 ²	26M	5.7G	82.7
LocalVMamba-S [25]	224 ²	50M	11.4G	83.7
SiMBA-S [24]	224 ²	15.3M	2.4G	81.7
SiMBA-B [24]	224 ²	22.8M	4.2G	83.5
SiMBA-L [24]	224 ²	36.6M	7.6G	84.4

the selective scanning mechanism of Mamba is adjusted for adapting the 1D operation to 2D images. Firstly, as zigzag scan depicted in Fig. 5, a continuous 2D scanning technique is utilized to ensure the spatial adjacency of tokens and prevent discontinuity. Secondly, a direction-aware updating technique is proposed to explicitly incorporate relative 2D position information into the selective scanning process.

B. Hybrid Mamba

1) *LocalMamba*: LocalMamba [25] addresses a significant limitation observed in the Vim [21] and VMamba [20] models, the disrupted dependencies among spatially local tokens during a single scanning process. To overcome this issue, as local sampling depicted in Fig. 5, LocalMamba divides the input image into multiple local windows to perform SSM in different directions as VMamba [20], while also maintaining the global SSM operations. Furthermore, LocalMamba implements a

TABLE II: Results of object detection and instance segmentation on MS COCO *mini-val* using Mask R-CNN [33] 1× schedule and 3× schedule. FLOPs are computed using input size 1280×800.

Mask R-CNN 1× schedule									
Backbone	Params	FLOPs	AP ^b	AP ^b ₅₀	AP ^b ₇₅	AP ^m	AP ^m ₅₀	AP ^m ₇₅	
ConvNets									
ResNeXt101-32x4d [34]	63M	340G	41.9	-	-	37.5	-	-	
ResNeXt101-64x4d [34]	102M	493G	42.8	-	-	38.4	-	-	
ConvNeXt-T [35]	48M	262G	44.2	66.6	48.3	40.1	63.3	42.8	
ConvNeXt-S [35]	70M	348G	45.4	67.9	50.0	41.8	65.2	45.1	
Transformers									
ViT-Adpt-T [36]	29M	349G	41.1	62.5	44.3	37.5	59.7	39.9	
ViT-Adpt-S [36]	49M	403G	44.7	65.8	48.3	39.9	62.5	42.8	
ViT-Adpt-B [36]	131M	883G	47.0	68.2	51.4	41.8	65.1	44.9	
PVT-Small [37]	44M	-	40.4	62.9	43.8	37.8	60.1	40.3	
PVT-Medium [37]	64M	-	42.0	64.4	45.6	39.0	61.6	42.1	
PVT-Large [37]	81M	-	42.9	65.0	46.6	39.5	61.9	42.5	
Swin-Tiny [6]	48M	264G	42.2	-	-	39.1	-	-	
Swin-Small [6]	69M	354G	44.8	-	-	40.9	-	-	
ViL-Tiny [38]	26M	145G	41.4	63.5	45.0	38.1	60.3	40.8	
ViL-Small [38]	45M	218G	44.9	67.1	49.3	41.0	64.2	44.1	
ViL-Medium [38]	60M	293G	47.6	69.8	52.1	43.0	66.9	46.6	
SSMs									
PlainMamba-Adpt-L1 [23]	31M	388G	44.1	64.8	47.9	39.1	61.6	41.9	
PlainMamba-Adpt-L2 [23]	53M	542G	46.0	66.9	50.1	40.6	63.8	43.6	
PlainMamba-Adpt-L3 [23]	79M	696G	46.8	68.0	51.1	41.2	64.7	43.9	
VMamba-T [20]	50M	270G	47.4	69.5	52.0	42.7	66.3	46.0	
VMamba-S [20]	64M	357G	48.7	70.0	53.4	43.7	67.3	47.0	
VMamba-B [20]	108M	485G	49.2	70.9	53.9	43.9	67.7	47.6	
EffVMamba-T [26]	11M	60G	35.6	57.7	38.0	33.2	54.4	35.1	
EffVMamba-S [26]	31M	197G	39.3	61.8	42.6	36.7	58.9	39.2	
EffVMamba-B [26]	53M	252G	43.7	66.2	47.9	40.2	63.3	42.9	
LocalVMamba-T [25]	45M	291G	46.7	68.7	50.8	42.2	65.7	45.5	
LocalVMamba-S [25]	69M	414G	48.4	69.9	52.7	43.2	66.7	46.5	
SiMBA-S [24]	60M	382G	46.9	68.6	51.7	42.6	65.9	45.8	
Mask R-CNN 3× schedule									
ConvNets									
ConvNeXt-T [35]	48M	262G	46.2	67.9	50.8	41.7	65.0	44.9	
ConvNeXt-S [35]	70M	348G	47.9	70.0	52.7	42.9	66.9	46.2	
Transformers									
ViT-Adpt-S [36]	48M	403G	48.2	69.7	52.5	42.8	66.4	45.9	
Swin-T [6]	48M	267G	46.0	68.1	50.3	41.6	65.1	44.9	
Swin-S [6]	69M	354G	48.2	69.8	52.8	43.2	67.0	46.1	
SSMs									
VMamba-T [20]	50M	270G	48.9	70.6	53.6	43.7	67.7	46.8	
VMamba-S [20]	70M	384G	49.9	70.9	54.7	44.2	68.2	47.7	
LocalVMamba-T [25]	45M	291G	48.7	70.1	53.0	43.4	67.0	46.4	
LocalVMamba-S [25]	69M	414G	49.9	70.5	54.4	44.1	67.8	47.4	

spatial and channel attention module before patch merging to enhance the integration of directional features and reduce redundancy. The LocalMamba block is illustrated in Fig. 4 (f). In addition, it adopts a strategy to select the most effective scan directions for each layer, thereby optimizing computational efficiency.

2) *EfficientVMamba*: EfficientVMamba [26] introduces the efficient 2D scanning (ES2D) technique, which employs atrous sampling of patches on the feature map to reduce computational burdens. The atrous sampling is illustrated in Fig. 5. ES2D is used to extract the global features, while a parallel

TABLE III: Results of semantic segmentation on ADE20K *val* using UperNet [39]. FLOPs are calculated using input size 512×2048 . ‘SS’ and ‘MS’ denote single-scale and multi-scale testing, respectively. MLN: multi-level neck.

Backbone	Crop Size	Params	FLOPs	mIoU (SS)	mIoU (MS)
ConvNets					
ResNet-50 [3]	512^2	67M	953G	42.1	42.8
ResNet-101 [3]	512^2	85M	1030G	42.9	44.0
ConvNeXt-T [35]	512^2	60M	939G	46.0	46.7
ConvNeXt-S [35]	512^2	82M	1027G	48.7	49.6
ConvNeXt-B [35]	512^2	122M	1170G	49.1	49.9
Transformers					
DeiT-S + MLN [40]	512^2	58M	1217G	43.8	45.1
DeiT-B + MLN [40]	512^2	144M	2007G	45.5	47.2
Swin-T [6]	512^2	60M	945G	44.4	45.8
Swin-S [6]	512^2	81M	1039G	47.6	49.5
Swin-B [6]	512^2	121M	1188G	48.1	49.7
SSMs					
Vim-Ti [21]	512^2	13M	-	41.0	-
Vim-S [21]	512^2	46M	-	44.9	-
PlainMamba-L1 [23]	512^2	35M	174G	44.1	-
PlainMamba-L2 [23]	512^2	55M	285G	46.8	-
PlainMamba-L3 [23]	512^2	81M	419G	49.1	-
VMamba-T [20]	512^2	62M	948G	48.3	48.6
VMamba-S [20]	512^2	82M	1039G	50.6	51.2
VMamba-B [20]	512^2	122M	1170G	51.0	51.6
EffVMamba-T [26]	512^2	14M	230G	38.9	39.3
EffVMamba-S [26]	512^2	29M	505G	41.5	42.1
EffVMamba-B [26]	512^2	65M	930G	46.5	47.3
LocalVim-T [25]	512^2	36M	181G	43.4	44.4
LocalVim-S [25]	512^2	58M	297G	46.4	47.5
LocalVMamba-T [25]	512^2	57M	970G	47.9	49.1
LocalVMamba-S [25]	512^2	81M	1095G	50.0	51.0
SiMBA-S [24]	512^2	62M	1040G	49.0	49.6

convolutional branch is used to extract the local features. Both feature types are then individually processed by a squeeze-and-excitation (SE) block. Collectively, the ES2D, the convolutional branch, and the SE block constitute the core components of the efficient visual state space (EVSS) block. The output of the EVSS block is the summation of the modulated global and local features. The EVSS block is shown in Fig. 3 (d). The EVSS blocks form the early stages of the EfficientVMamba, whereas the EfficientNet blocks invertedly form the later stages.

3) *SiMBA*: SiMBA [24] aims to address the instability issue of Mamba scaling to large networks on vision datasets. It proposes a new channel modeling technique termed EinFFT and uses Mamba for sequence modeling. In other words, SiMBA block is comprised of a Mamba block and an EinFFT block, both interleaved with LN layer, dropout, and residual connections.

C. Key Improvements

1) *Backbone*: To process 2D images, they are first converted into sequences of visual tokens via a stem module, typically comprising a convolution layer followed by a linear projection layer. The addition of positional embeddings is optional, as the SSM operation inherently possesses causal

properties. The inclusion of a class token is also optional. Existing approaches process image sequences by treating them as either 1D or 2D structures for the SSM transformations and convolution operations in the Mamba-based blocks. Given the integral role of scanning techniques in these processes, we will systematically categorize and delve into these approaches in greater detail in the subsequent section. In this section, we differentiate between hierarchical and non-hierarchical Mamba-based architectures. Hierarchical architectures, akin to widely used CNNs [1], [2] and some versions of ViTs [6], [42], incorporate down-sampling techniques to construct layered representations. An example of such a hierarchical architecture is VMamba [20]. In contrast, non-hierarchical architectures consist of stacks of multiple identical Mamba-based blocks without layered differentiation. A typical example of a non-hierarchical architecture is Vim [21].

2) *Scan*: The selective scanning mechanism is the key component of Mamba. However, its original design for 1D causal sequences poses challenges when adapting it to 2D non-causal images. Considerable research efforts are devoted to addressing these challenges. In the following section, we categorize and discuss these efforts into three main groups, scan mode, scan axis, and scan continuity. This categorization is based on the objectives of the scanning techniques. The scan mode addresses the non-causal characteristics of visual data; the scan axis deals with the high dimensionality inherent in visual data; the scan continuity considers the spatial continuity of the patches along the scanning path; the scan sampling divides the full image into sub-images. The illustration of these four groups is shown in Fig. 5.

1. **Scan Mode**: After unfolding the visual data into 1D sequences, different scan modes can be employed to handle the non-causal nature of these sequences. We first denote the original selective scanning technique, which operates in a single direction, as **SD**. In [21], bi-directional sequence modeling is employed to enhance the receptive fields reciprocally. We refer to this approach as **BD**. In addition to the two common scan modes, supplementary shuffle or reordering strategies can be employed for scanning. We denote the utilization of these strategies with the labels **+Shuffle** or **+Reordering**, respectively.

2. **Scan Axis**: Despite their non-causal properties, visual data differ from typical sequences by possessing 2D or higher-dimensional spatial information that encapsulates both local and global contexts. Current approaches unfold visual data along various axes to thoroughly integrate this spatial information. For instance, the scanning axes for a 2D image typically include the horizontal, vertical, left diagonal, and right diagonal, designated as **H**, **V**, **LD**, and **RD**, respectively. For 3D visual data, the axes also involve depth or temporal dimensions, denoted as **D**.

3. **Scan Continuity**: Alternative techniques are employed to handle the 2D spatial information in visual data. Some approaches, inspired by the ViT [4], flatten images into sequences. This technique, however, may lead to spatial discontinuities between rows or columns; we refer to this technique as **Raster** scanning. In contrast, other approaches ensure continuous scanning to maintain spatial continuity among

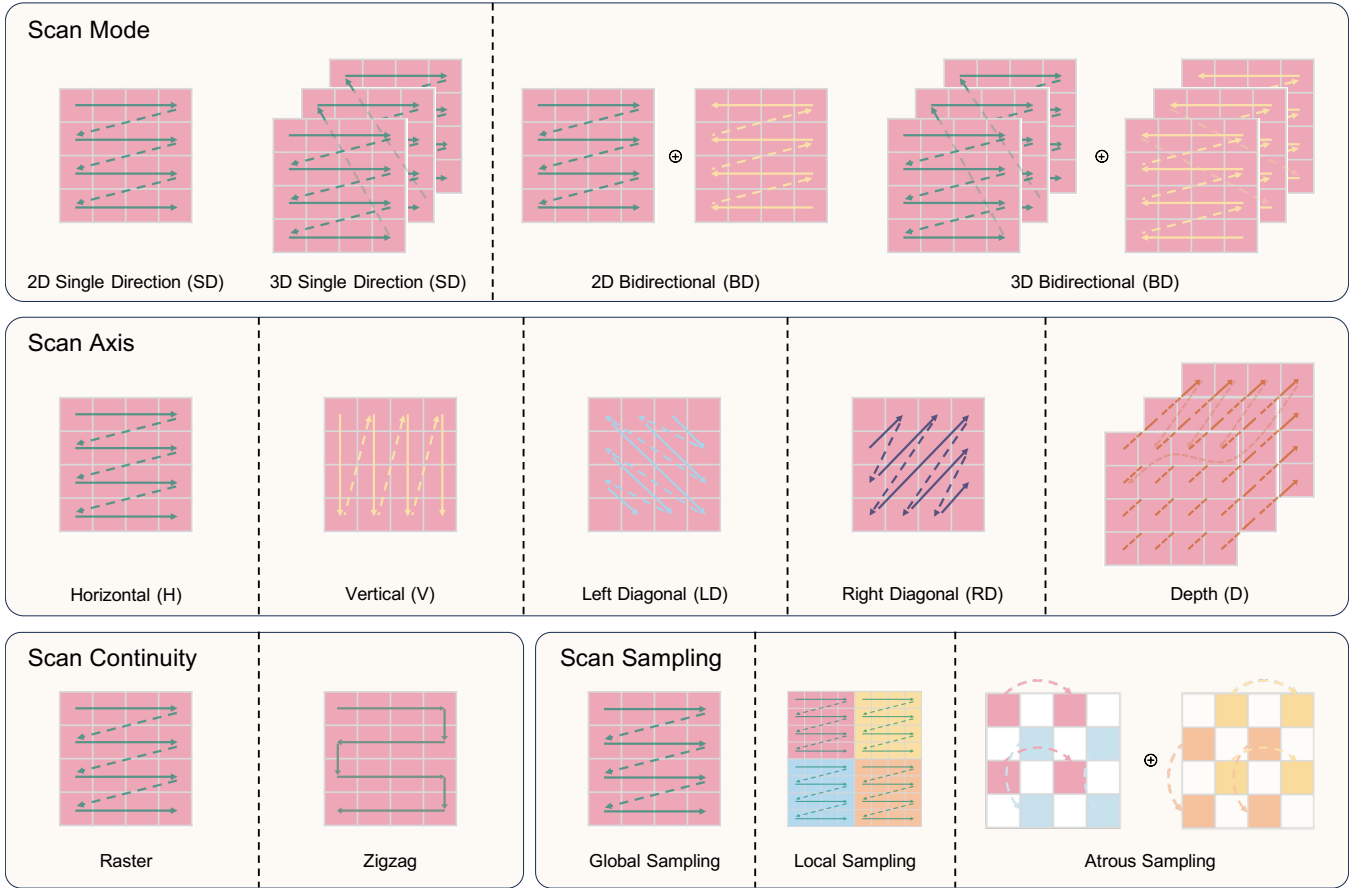


Fig. 5: Scan techniques, categorized into four groups, i.e. scan mode, scan axis, scan continuity, and scan sampling.

adjacent tokens, a technique we denote as **Zigzag**.

4. **Scan Sampling:** We introduce sampling techniques that divide the image into sub-images for scanning using **Local Sampling** or **Atrous Sampling**. Notably, within these sub-images, different combinations of the former three groups of scanning techniques can be applied, allowing for diverse processing approaches without the necessity for uniformity across all sub-images. The comparison of the obtained sub-images and the original full image, which is denoted as **Global Sampling**, is illustrated.

These four groups of scanning techniques are interoperable and can be synergistically combined to enhance visual data analysis.

3) **Block:** Different combinations of the previously mentioned scanning techniques and the selective SSM transformation form various blocks, which are integral to Mamba-based architectures. In discussing the visual Mamba backbone networks, we provide an overview of these blocks, with detailed illustrations presented in corresponding figures. These figures also validate the logic behind our categorization of scanning techniques. These blocks are extensively utilized in the application approaches that will be detailed in the subsequent section. For clarity, the original Mamba block is referred to simply as **Mamba**. Representative blocks are denoted by names such as **VSS** and **Vim**. Modifications to these blocks are indicated by an asterisk (*) and labels such as **+CNN** signify

the integration of CNN-like features. Fig. 3 and Fig. 4 illustrate a suite of visual Mamba blocks, including Vim Block, VSS Block, EVSS Block, PlainMamba Block, LocalMamba Block, and Mamba-ND Block. The Mamba Block is also included to facilitate a direct comparison, highlighting the evolutionary design of these blocks in the visual domain.

In this section, we present the performance of various visual Mamba backbone networks on standard benchmarks in Table. I, Table. II, and Table. III: classification on ImageNet-1K [43], object detection and instance segmentation on the MS COCO [44] via Mask R-CNN [33], and semantic segmentation on ADE20K [45] utilizing UperNet [39].

IV. APPLICATION

In this section, we systematically categorize and discuss the diverse applications of Mamba in the field of computer vision. The categorization scheme, along with an overview of the relevant literature reviewed in this survey, is presented in Fig. 6.

A. Image

1) **Classification:** In addition to the backbones [20], [21] conducting image classification for representation learning, Mamba-ND [22] introduces a novel approach for processing multi-dimensional data by alternately unraveling the input data across different dimensions following row-major orderings.

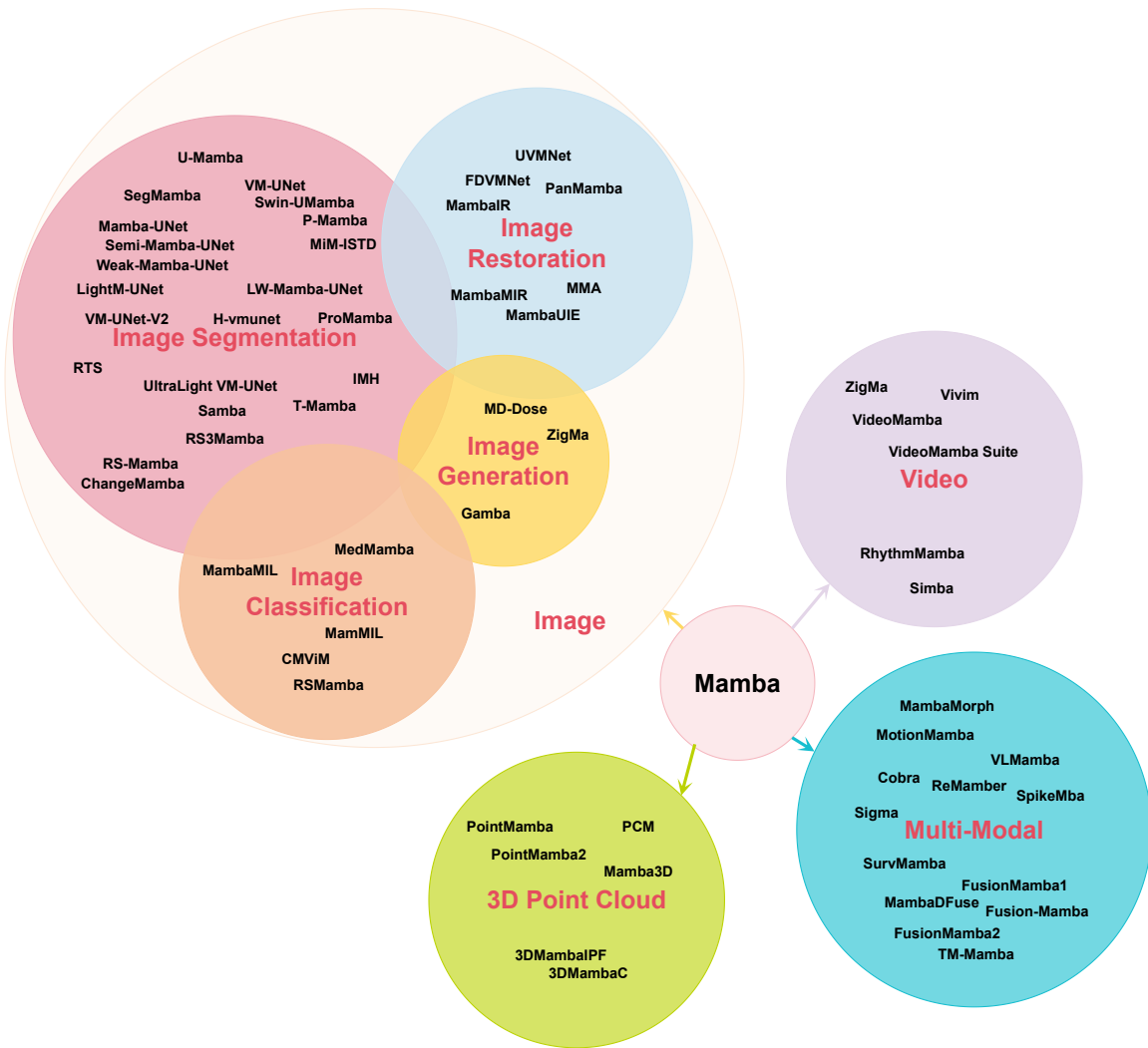


Fig. 6: Applications of Mamba across various vision domains.

This technique has demonstrated superior performance with significantly fewer parameters compared to transformer-based methods in the context of natural image classification. Meanwhile, Mamba-ND can be easily extended to several tasks such as video action recognition and 3D segmentation involving multi-dimensional data. The scalability of Mamba-based architectures to larger patch sequences has led to their adoption in the analysis of high-resolution images (e.g., Whole Slide Images and Remote Sensing Images) and high-dimensional images (e.g., 3D Medical Images) for recognition purposes.

Specifically, both MamMIL [47] and MambaMIL [48] utilize Mamba, which is capable of effective long sequence modeling, to enhance Multiple Instance Learning (MIL) for computational pathology analysis. MamMIL employs a bidirectional state space model similar to Vim and a 2D context-aware block [83] to enhance instance aggregation. MambaMIL introduces a novel approach named Sequence Reordering Mamba (SR-Mamba), which is sensitive to the order and distribution of instances and leverages the valuable information embedded within these long sequences. CMViM [49] proposes a contrastive masked Vim autoencoder tailored for 3D multi-

modal data to facilitate Alzheimer’s disease (AD) recognition. This approach incorporates Vim into the masked autoencoder, enabling the effective reconstruction of 3D masked multi-modal data and capturing the inherent long-range dependencies present in 3D medical data. RSMamba [50] introduces a position-sensitive dynamic multi-path activation mechanism, encompassing forward, backward, and shuffle paths, to extract precise semantic cues for accurate scene discrimination. MedMamba [46] introduces the SS-Conv-SSM module, which combines the local feature extraction ability of convolutional layers with the ability of SSM to capture long-range dependency.

2) *Segmentation*: Segmentation continues to be a vital and prominent area of study within the computer vision field, holding immense value for diverse real-world applications. Recent advancements in segmentation techniques have witnessed remarkable achievements through the utilization of CNN-based models and transformer-based models. CNN-based approaches excel in capturing local features via their convolution operations, whereas transformer-based methods demonstrate exceptional prowess in comprehending global

TABLE IV: The Mamba-based methods in Image-Level Vision Tasks. The abbreviations of Backbone here are VSS: Vision State Space Module, Vim: Vision Mamba, *: modification. The abbreviations of Data here are CBCT: Cone Beam Computed Tomography, CXR: Chest X-Ray, CT: Computed Tomography, Derm: Dermatoscope, Echo: Echocardiograms, Endo: Endoscopic Images, FMRI: Fast Magnetic Resonance Imaging, Micro: Microscopy Images, MRI: Magnetic Resonance Imaging, OCT: Optical Coherence Tomography, Path: Pathology, PET: Positron Emission Tomography, Skin: Skin Lesion Images, Spleen: Spleen Images, SVCT: Sparse-view Computed Tomography, UI: Ultrasound Images. The abbreviations of Task here are CLS: Classification, DET: Detection, SEG: Segmentation.

Methods	Backbone	Data	Task	Scan	Continuity	Time	Code
Image Classification							
Mamba-ND [22]	Mamba*	Natural Images	2D Natural Images CLS	BD (H/V/D)	Raster	2024/02/08	✓
MedMamba [46]	VSS*	2D Medical Images (Skin/UI/CXR/Endo/OCT/CT/Micro/Path/Derm)	2D Medical Image CLS	BD (H/V)	Raster	2024/03/06	✓
MamMIL [47]	Vim*	Whole Slide Images	Cancer Subtyping	BD (H)	Raster	2024/03/08	✓
MambaMIL [48]	Mamba*	Whole Slide Images	Cancer Subtyping/Survival Prediction	SD (H) + Reordering	Raster	2024/03/11	✓
CMViM [49]	Vim	3D Medical Images (MRI & PET)	3D Medical Image CLS	BD (H)	Raster	2024/03/25	✓
RSMamba [50]	Mamba	Remote Sensing Images	Remote Sensing Images CLS	BD (H/V) + Shuffle	Raster	2024/03/28	✓
Image Segmentation							
U-Mamba [51]	Mamba*	2D/3D Medical Images (Endo/Micro/CT/MRI)	2D/3D Medical Image SEG	SD (H)	Raster	2024/01/09	✓
SegMamba [52]	Mamba*	3D Medical Images (CT/MRI)	3D Medical Image SEG	BD (H) + SD (D)	Raster	2024/01/24	✓
VM-UNet [53]	VSS	2D Medical Images (Skin/CT)	2D Medical Image SEG	BD (H/V)	Raster	2024/02/05	✓
Swin-UMamba [54]	VSS	2D Medical Images (Endo/Micro/MRI)	2D Medical Image SEG	BD (H/V)	Raster	2024/02/05	✓
Mamba-UNet [55]	VSS	2D Medical Images (CT/MRI)	2D Medical Image SEG	BD (H/V)	Raster	2024/02/07	✓
Mamba-ND [22]	Mamba*	3D Medical Images (CT)	3D Medical Images SEG	BD (H/V/D)	Raster	2024/02/08	✓
Semi-Mamba-UNet [56]	VSS	2D Medical Images (MRI)	2D Medical Image SEG	BD (H/V)	Raster	2024/02/11	✓
P-Mamba [57]	Vim	2D Medical Images (Echo)	2D Medical Image SEG	BD (H)	Raster	2024/02/13	✓
Weak-Mamba-UNet [58]	VSS	2D Medical Images (MRI)	2D Medical Image SEG	BD (H/V)	Raster	2024/02/16	✓
MIM-ISTD [59]	VSS*	Infrared Images	Infrared Image SEG	BD (H/W)	Raster	2024/03/04	✓
LightM-UNet [60]	VSS	2D/3D Medical Images (CXR/CT)	2D/3D Medical Image SEG	BD (H/W)	Raster	2024/03/08	✓
LW-Mamba-UNet [61]	Vim*	2D/3D Medical Images (MRI/CT)	2D/3D Medical Image SEG	BD (H)	Raster	2024/03/12	✓
VM-UNet-V2 [62]	VSS	2D Medical Images (Skin/Endo)	2D Medical Image SEG	BD (H/V)	Raster	2024/03/14	✓
H-vmunet [63]	VSS*	2D Medical Images (Skin/Spleen/Endo)	2D Medical Image SEG	BD (H/V)	Raster	2024/03/14	✓
ProMamba [64]	Vim	2D Medical Images (Endo)	2D Medical Image SEG	BD (H)	Raster	2024/03/20	✓
RTS [65]	VSS*	2D Medical Images (Endo/Micro/2D CT/2D MRI)	2D Medical Image SEG	BD (H/V)	Raster	2024/03/26	✓
IMH [66]	VSS	2D Medical Images (2D MRI)	2D Medical Image SEG	BD (H/V)	Raster	2024/03/26	✓
UltraLight VM-UNet [67]	VSS*	2D Medical Images (Skin)	2D Medical Image SEG	BD (H/V)	Raster	2024/03/29	✓
T-Mamba [68]	Vim*	3D Medical Images (CBCT)	3D Medical Image SEG	BD (H) + Fourier Transform	Raster	2024/04/01	✓
Samba [69]	Mamba*	Remote Sensing Images	Semantic SEG	SD (H)	Raster	2024/04/02	✓
RS3Mamba [70]	VSS	Remote Sensing Images	Semantic SEG	BD (H/V)	Raster	2024/04/03	✓
RS-Mamba [71]	Mamba*	Remote Sensing Images	Semantic SEG/Change DET	BD (H/V/LD/RD)	Raster	2024/04/03	✓
ChangeMamba [72]	VSS	Remote Sensing Images	Change DET/Building Damage Assessment	BD (H/V)	Raster	2024/04/04	✓
Image Generation							
MD-Dose [73]	Mamba	2D Medical Images (CT)	Radiation Dose Prediction	SD (H)	Raster	2024/03/13	✓
ZigMa [74]	Mamba*	Natural Images	Image Generation	BD (H/V)	Zigzag	2024/03/20	✓
Gamba [75]	Mamba*	Natural Images	3D Reconstruction	SD (H)	Raster	2024/03/27	✓
Image Restoration							
UVMNet [76]	Mamba*	Natural Images	Dehazing/Low Light Enhancement/Draining	SD (H) + Channel	Raster	2024/02/06	✓
FDVMNet [77]	Mamba*	2D Medical Images (Endo)	Endoscopic Exposure Correction	SD (H)	Raster	2024/02/09	✓
PanMamba [78]	VSS*	Remote Sensing Images	Remote Sensing Images Pan-sharpening	SD (H)	Raster	2024/02/19	✓
MambaIR [79]	VSS*	Natural Images	Super-resolution/Denoising	BD (H/V)	Raster	2024/02/23	✓
MambaMIR [80]	VSS*	3D Medical Images (FMRI/SVCT)	Medical Image Restoration	BD (H/V)	Raster	2024/02/28	✓
MMA [81]	Vim*	Natural Images	Super-resolution	BD (H)	Raster	2024/03/13	✓
MambaUIE [82]	VSS*	Underwater Images	Underwater Image Enhancement	BD (H/V)	Raster	2024/04/28	✓

context through the utilization of self-attention mechanisms. However, one limitation of transformer-based methods is the quadratic growth in computational complexity of self-attention as the input size increases. Especially for high-resolution images or high-latitude images, the Transformer architecture and its integral attention layer are limited in their ability to model anything beyond a finite window and exhibit quadratic complexity, resulting in sub-optimal performance.

Recent advances [51]–[55], [57] based on Mamba have appeared in the medical domain, encompassing diverse data such as 2D and 3D medical images. Several methods [53]–[56] directly replace CNN-blocks of U-Net architecture with Mamba like-blocks [19]–[21]. U-Mamba [51] is the first effective attempt to apply Mamba in the field of medical image segmentation. U-Mamba designs a hybrid CNN-SSM block by integrating the local feature extraction power of convolutional layers with the abilities of SSMs for capturing the long-range dependency and follows the encoder-decoder network structure to capture both local features and long-range contexts. SegMamba [52] introduces a Gated Spatial Convolution (GSC) to extract the spatial relationship, followed

by a Tri-orientated Spatial Mamba by adding an inter-slice path for 3D data. Both VM-UNet [53], Swin-UMamba [54] and Mamba-UNet [55] employ VSS as a foundation block to capture extensive contextual information. Mamba-UNet [55] is further enhanced through the incorporation of a semi-supervised setting [56] and a weak-supervised setting [58]. P-Mamba [57], LW-Mamba-UNet [61], Pro-Mamba [64] and T-Mamba [68] employ Vim as foundation block and design effective components to enhance vanilla Vim. Meanwhile, several Mamba-based methods [51], [53], [54], [60], [61], [63] conduct extensive experiments on both 2D and 3D medical datasets, which demonstrates the efficacy of Mamba architecture for both 2D and 3D medical images.

Recent advances [59], [69]–[72] based on Mamba architecture have appeared in the various datasets, encompassing infrared images and remote sensing images, showcasing their versatility and effectiveness in these domains. MIM-ISTD [59] proposes a novel Mamba-in-Mamba structure, where it employs Outer Mamba to explore the global information and utilizes Inner Mamba to further explore the local information within each visual patch. Samba [69] replaces the Multi-Head

Self-Attention block with vanilla Mamba to efficiently capture global semantic information. RS3Mamba [70] utilizes VSS blocks to construct an auxiliary branch, providing additional global information to the convolution-based main branch. RS-Mamba [71] introduces an Omni-directional Selective Scan Module based on Mamba, which globally models the context of images in multiple directions, capturing large spatial features from various directions. ChangeMamba [72] adopts the cutting-edge VSS architecture as the encoder and proposes spatial-temporal relationship modeling mechanisms based on VSS blocks to achieve spatial-temporal interaction of multi-temporal features.

3) *Generation*: Intuitively, applying the Mamba architecture to a series of generation tasks to achieve sufficient long sequence interactions has the potential to achieve impressive performance.

MD-Dose [73] introduces a novel diffusion model based on the Mamba architecture for predicting radiation therapy dose distribution in thoracic cancer patients. ZigMa [74] leverages spatial continuity to maximally incorporate the inductive bias from visual data. Specifically, it utilizes zigzag-scan scheme with various directions to efficiently incorporate tokens to maximize the potential of long sequence modeling within the Mamba block. Gamba [75] introduces GambaFormer to process 3D Gaussian Splatting by utilizing the newly proposed Gaussian Mamba.

4) *Image Restoration*: Recently, the Mamba architecture has also been widely used in several low-level tasks, including image dehazing [76], exposure correction [77], pan-sharpening [78], super-resolution [79], [81], denoising [79], medical image reconstruction [80] and underwater image enhancement [82].

UVMNet [76] integrates the novel Bi-SSM module into the U-Net architecture for image dehazing tasks. The Bi-SSM module scrolls the feature maps over the spatial domain and channel domain, and utilizes an attention map, derived from the SSM and the softmax function, to enhance the feature map. FDVMNet [77] introduces a C-SSM block by combining convolution, SSM, cross-attention and shortcut as a basic cell, and utilizes two paths to deal with the phase and amplitude of the frequency domain information respectively. PanMamba [78] proposes channel swapping Mamba and cross-modal Mamba, designed for efficient information exchange and fusion between low-resolution multi-spectral and high-resolution panchromatic images. MambaMIR [80] introduces an Arbitrary-Masked State Space (AMSS) block based on VSS by adopting an arbitrary-mask mechanism to leverage the scanning redundancy. MMA [81] introduces the MMA block by combining channel attention blocks and Vim blocks in parallel. The MMA block is utilized to replace Multi-head Self-Attention in the conventional transformer block to further enlarge the overall activated areas.

The extraction of local fine-grained features plays a critical role in tackling low-level image tasks, and these essential features are not present in the vanilla Mamba. It is straightforward to hold the opinion that incorporating a convolution-based module with SSM can help Mamba-based methods get a better visual representation. MambaIR [79] introduces a

Residual State Space block with both local convolution-based enhancement and channel attention to improve the vanilla Mamba for image super-resolution and image denoising tasks, which takes advantage of the local pixel similarity and reduces the channel redundancy. MambaUIE [82] is specifically developed to improve the visual quality of underwater images degraded due to light absorption and scattering. It proposes a Dynamic Interaction-Visual State Space Block (DI-VSS) by combining convolution in parallel with VSS and integrating a Dynamic Interaction Block (DIB) for local capture capability and efficient long-range modeling.

B. Video

Video understanding is one of the fundamental directions in computer vision research. The primary goal of video understanding is to effectively master spatio-temporal representations across long contexts. Mamba excels in this domain with its selective state space model, which achieves a balance between maintaining linear complexity and enabling effective long-term dynamic modeling. This innovative approach has catalyzed its widespread adoption in diverse video analysis tasks such as video object segmentation [84], video action recognition [22], video generation [74] and representation learning [85], [86].

Vivim [84] introduces a Mamba-based framework for medical video object segmentation, featuring a novel temporal mamba block with spatiotemporal selective scanning. MambaND [22] extends the Selective State Model to higher dimensions, unraveling the input data across various dimensions in row-major order. In addition to the 2D image tasks previously discussed, it also explores mamba's effectiveness in video action recognition tasks. VideoMamba [85] extends Vim's original 2D scan into different bidirectional 3D spatiotemporal scans to build a purely SSM-based model for video understanding. It showcases the scalability of the Mamba backbone in the visual domain through the use of self-distillation pre-training techniques. VideoMamba sets new benchmarks for video understanding across short-term, long-term, and multi-modal video tasks, providing a scalable and efficient solution for comprehensive analysis of video content. Different from VideoMamba, VideoMamba Suite [86] does not propose a novel method but focuses more on assessing whether Mamba can serve as a viable alternative to Transformers in the video understanding domain. It leverages Mamba in four distinct roles: temporal models, temporal modules, multi-modal interaction models, and space-time sequence models to reveal Mamba's effectiveness in video understanding and to emphasize its key characteristics. VideoMamba Suite demonstrates Mamba's ability to efficiently handle complex spatial-temporal dynamics, showcasing both superior performance and favorable efficiency-performance trade-offs. Zigma [74] develops several spatially continuous, space-filling 2D scanning schemes for image generation. Additionally, it factorizes the 3D Mamba model into 2D and 1D Zigzag Mamba to enhance the integration of spatial and temporal information in video generation. RhythmMamba [87] design multi-temporal Mamba as well as frequency domain feed-forward channel

TABLE V: The Mamba-based methods in Video-Level/Multi-Modal/Point Cloud Vision Tasks. The abbreviations of Backbone here are VSS: Vision State Space Module, Vim: Vision Mamba, *: modification. The abbreviations of Data here are CT: Computed Tomography, HISR Images: High-resolution Multi-spectral Images, LRMS Images: Low-resolution Multi-spectral Images, MRI: Magnetic Resonance Imaging, PET: Positron Emission Tomography, SPECT: Single-photon Emission Computed Tomography. The abbreviations of Task here are CLS: Classification, DET: Detection, SEG: Segmentation.

Methods	Backbone	Data	Task	Time	Code
Video					
Vivim [84]	Vim*	Ultrasound Videos, Endoscopic Videos	Video Object SEG	2024/01/25	✓
Mamba-ND [22]	Mamba	Natural Videos	Video Action Recognition	2024/02/08	✓
VideoMamba [85]	Vim*	Natural Videos	Action CLS, Long-form Video Understanding, Text-to-Video Retrieval	2024/03/11	✓
VideoMamba Suite [86]	Vim*	Natural Videos	Action Localization, Action anticipation, Action Recognition, Video Captioning Video Grounding, Video Question Answering, Multi-instance Retrieval	2024/03/14	✓
ZigMa [74]	Mamba*	Natural Videos	Video Generation	2024/03/20	✓
RhythmMamba [87]	Mamba*	Facial Videos	rPPG Prediction	2024/04/09	✓
Simba [88]	Mamba	Skeletal Action Videos	Skeletal Action Recognition	2024/04/11	
Multi-Modal					
MambaMorph [89]	Mamba	MRI & CT	MRI-CT Registration	2024/01/24	✓
MotionMamba [90]	Mamba*	Motion Data & Textual Descriptions	Motion Generation	2024/03/12	✓
VLMamba [91]	VSS*	Natural Images & Text	Visual Question Answering, Multimodal Reasoning, Multimodal Scene Understanding	2024/03/20	✓
Cobra [92]	Mamba	Natural Images & Text	Visual Question Answering, Multimodal Reasoning	2024/03/21	✓
ReMamber [93]	VSS*	Natural Images & Text	Referring Image Segmentation	2024/03/26	
SpikeMba [94]	Vim*	Natural Videos & Text	Temporal Video Grounding	2024/04/01	
Sigma [95]	VSS*	RGB Images & Thermal/Depth Images	Semantic SEG	2024/04/05	✓
SurvMamba [96]	Vim*	WSIs & Gene	Survival Prediction	2024/04/11	
FusionMamba1 [97]	VSS*	HISR Images & LRMS Images	Pansharpening	2024/04/11	✓
MambaDFuse [98]	Mamba*	RGB Images & Thermal Images, MRI & CT/PET/SPECT	Infrared-visible Image Fusion, Medical Image Fusion, Object DET	2024/04/12	
Fusion-Mamba [99]	VSS*	RGB Images & Thermal Images	Object DET	2024/04/20	
FusionMamba2 [100]	VSS*	RGB Images & Thermal Images, MRI & CT/PET/SPECT	Infrared-visible Image Fusion, Medical Image Fusion	2024/04/14	✓
TM-Mamba [101]	Vim*	Motion Sequence & Text	Human Motion Grounding	2024/04/17	
3D Point Cloud					
PointMamba [102]	VSS*	3D Point Cloud Data	Object CLS, Part SEG	2024/02/16	✓
PCM [103]	Vim*	3D Point Cloud Data	Object CLS, Part SEG, Semantic SEG	2024/03/01	✓
PointMamba2 [104]	Vim*	3D Point Cloud Data	Object CLS, Semantic SEG	2024/03/11	✓
3DMambaPF [105]	Mamba	3D Point Cloud Data	Point Cloud Filtering	2024/04/08	
3DMambaC [106]	Mamba*	3D Point Cloud Data	Point Cloud Completion	2024/04/10	
Mamba3D [107]	Vim*	3D Point Cloud Data	Object CLS, Part SEG	2024/04/23	

interacting to enable Mamba to capture the quasi-periodic patterns of remote photoplethysmography (rPPG). This study also explores the performance of RhythmMamba under long-time series inputs, demonstrating its robust performance over arbitrary length videos. Simba [88] leverages Mamba within a novel encoder-decoder architecture with a Shift-GCN backbone to address the challenge of efficiently modeling long sequences inherent in skeleton action recognition tasks.

C. Multi-Modal

Multi-modal tasks play a crucial role in the field of CV, as they facilitate the integration of diverse information sources to enrich the comprehension and analysis of visual data. The objective of these tasks is to aggregate a multitude of modalities, encompassing textual and visual information, RGB images with additional components such as depth or thermal images, and various forms of medical imaging data. However, a significant challenge in achieving multi-modal objectives lies in effectively capturing the correlations between different modalities. Recently, several methods employ Mamba architecture for numerous multi-modal tasks, including multi-modal large language model [91], [92], multi-modal registration [89], Referring Image Segmentation [93], Temporal Video Grounding [94], Semantic Segmentation [95], [98]–[100], Motion Generation [90] and medical applications [96], [98], [100].

MambaMorph [89] integrates Mamba block into the registration encoder for efficient long-range correspondence modeling. Motion Mamba [90] introduces a diffusion-based generative system, incorporating two modules based on the vanilla

Mamba, namely Hierarchical Temporal Mamba (HTM) and Bidirectional Spatial Mamba (BSM). HTM blocks are tasked with processing temporal motion data, aiming to enhance motion consistency across frames. BSM blocks are engineered to bidirectionally capture the channel-wise flow of hidden information within the latent pose representations. VLMamba [91] replaces the transformer-based backbone language model such as LLama [108] with the pre-trained Mamba language model. Meanwhile, it introduces the Multi-Modal Connector, comprising a Vision Selective Scan (VSS) module and two linear layers. Cobra [92] proposes a linear computational complexity multi-modality large language model, which utilizes DINOv2 [109] and SigLIP [110] as vision encoder and directly employs Mamba language model as the backbone. ReMamber [93] proposes Mamba Twister block, containing VSS block to extract vision feature and twister block to inject the textual information into the visual modality. Each twister block explicitly captures the fine-grained interactions and generates a hybrid feature cube. This cube is processed through two consecutive SSMs scanning along channel and spatial dimensions to enhance the channel interactions for the effective fusion of multi-modal data. SpikeMba [94] integrates the Spiking Neural Networks and SSMs to capture the fine-grained relationships of multi-modal features. For Mamba-based components, Contextual Moment Reasoner based on Vim-like block takes visual features and text features as input and gates both features by a same activation value. Meanwhile, Multi-modal Relevant Mamba utilizes spiking sequences to gate the contextually enriched multi-modal features enhanced by SSM. Sigma [95] introduces a siamese Mamba network

for multi-modal semantic segmentation, where it employs VSS blocks to extract visual features of different modalities during the encoder phase and proposes the Channel-Aware VSS block by adding average pooling operation and max pooling operation upon VSS block during the decoding phase. For the feature fusion modules, Cross Mamba Block (CroMB) employs a cross-multiplication mechanism to enhance the features with one another, and Concat Mamba Block (ConMB) applies the SSM to concatenated features to obtain the fusion result. SurvMamba [96] proposes the Hierarchical Interaction Mamba (HIM) to facilitate efficient intra-modal interactions at different granularities, and the Interaction Fusion Mamba to aggregate the cascaded multi-modal features, thereby capturing more detailed local features as well as rich global representations for comprehensive fusion. FusionMamba1 [97] incorporates VSS blocks into two U-shaped networks for extracting spatial and spectral features, and proposes the FusionMamba block by expanding SSM to accommodate dual inputs. MambaDFuse [98] proposes a Mamba-based Dual-phase Fusion model, including Dual-level Feature Extraction, Dual-phase Feature Fusion and Fused Image Reconstruction. Fusion-Mamba [99] proposes a Fusion-Mamba block to map cross-modal features into a hidden state space for interaction, thereby reducing disparities between cross-modal features and enhancing the representation consistency of fused features. FusionMamba2 [97] proposes a dynamic feature enhancement method based on Mamba, which integrates VSS block with dynamic convolution and channel attention. TM-Mamba [101] takes motion sequence and related text query as input, and utilizes stacked Text-controlled Motion Mamba (TM-Mamba) to integrate multi-modal information. The TM-Mamba employs VSS block, and utilizes the text-controlled selection mechanism to dynamically incorporate global temporal information based on text query.

D. Point Cloud

Point cloud is a fundamental 3D representation, which provides continuous spatial position information with 3D coordinates. The intrinsic disorder and irregularity natures of point cloud have been a challenge in 3D vision. Inspired by the linear complexity and global modeling capabilities of Mamba, several general SSM-based backbones [102]–[107] have been investigated in the field of point cloud processing.

PointMamba [102] directly employs VSS blocks as encoder and proposes a reordering strategy to enhance SSM’s global modeling ability by providing a more logical geometric scanning order. PCM [103] incorporates geometry affine block and Vim block as basic block, and proposes Consistent Traverse Serialization (CTS) to serialize point clouds into 1D point sequences while ensuring the spatial continuity. Specifically, CTS yields six variants by permuting the order of 3D coordinates, resulting in comprehensively observing point cloud data. PointMamba [102] employs Vim for long sequence modeling and introduces the octree-based ordering mechanism to generate input sequences for obtaining the causality of raw input points. 3DMambaIPF [105] incorporates Mamba architecture to sequentially handle extensive point clouds from

large scenes, and integrates a robust and fast differentiable rendering loss to constrain the noisy points around the surface. 3DMambaC [106] introduces a HyperPoint Generation module to produce the new shape representation-Hyperpoints, which includes Mamba Encoder for enhancing the sampled point features and predicts Hyperpoints. Mamba3D [107] employs a bidirectional SSM with channel flipping, and introduces Local Norm Pooling (LNP) block to extract local geometric features.

V. CHALLENGES

In this section, we explore the challenges associated with the untapped potential of the Mamba in the visual domain. We aim to identify key areas where Mamba’s capabilities can be extended and optimized, contributing to the ongoing evolution of visual Mamba.

A. Algorithm

1) *Scalability and Stability*: Currently, the Mamba architecture exhibits stability challenges when applied to large-scale datasets such as ImageNet. The underlying causes of Mamba’s instability upon scaling to more extensive network configurations remain unclear. This instability frequently leads to vanishing or exploding gradients within the Mamba framework [24], which impedes its deployment in large-scale visual tasks.

2) *Causality Issues*: Given that the Mamba model is initially designed for causal sequential data, adapting its selective scanning technique for non-causal visual data presents significant challenges. Current approaches address this by employing scanning techniques like bi-directional scanning, where both forward and backward scans are utilized to mutually compensate for the inherent limitations of one-directional scanning in receptive fields. However, this remains an unresolved issue that continues to present challenges.

3) *Spatial Information*: The inherently 1D nature of Mamba’s selective scanning technique presents challenges when applied to 2D or higher-dimensional visual data, as it can lead to a loss of critical spatial information. To address this limitation, current approaches often unfold image patches from various directions, thereby allowing the integration of spatial information across multiple dimensions. Nevertheless, this issue remains an open problem that requires further investigation.

4) *Redundancy and Computation*: The bi-directional scanning approach and the use of multiple scanning directions, as previously discussed, can lead to significant information redundancy and an increase in computational demands. These may decrease the model performance and reduce the advantage of Mamba’s linear complexity. According to research findings [111], GPU consumption for the Mamba model does not consistently demonstrate a reduction compared to the Transformer model. This represents an important challenge and warrants further investigation.

B. Application

1) *Interpretability*: Some studies have provided experimental evidence to elucidate the mechanisms underlying the Mamba model in NLP, focusing on its in-context learning capabilities [112], [113] and factual recall capabilities [114]. Additionally, other works [115] have laid theoretical foundations for Mamba’s applications in NLP. Despite these advancements, explaining why Mamba performs effectively on visual tasks remains challenging. In [116], the authors reinterpret Mamba layers as self-attention mechanisms, thereby shedding light on its functionality both empirically and theoretically. However, the distinct learning characteristics of visual Mamba and its parallels with other foundational models, such as RNNs, CNNs, and ViTs, still demand deeper interpretation.

2) *Generalization and Robustness*: According to findings in [117], the hidden states in Mamba are likely to accumulate or even amplify domain-specific information, which can adversely affect its generalization performance. Moreover, the 1D scanning strategies inherent to the model may inadvertently capture domain-specific biases, and current scanning techniques often fail to address the need for domain-agnostic information processing. Research presented in [118] demonstrates VMamba’s [20] strengths in adversarial resilience and general robustness. However, it also identifies limitations in scalability when dealing with these tasks. The study includes white-box attacks on VMamba to examine the behavior of its novel components under adversarial conditions. The findings indicate that while parameter Δ exhibits robustness, parameters \mathbf{B} and \mathbf{C} are susceptible to attacks. This differential vulnerability among parameters contributes to VMamba’s scalability challenges in maintaining robustness. Furthermore, the results reveal that VMamba exhibits particular sensitivity to interruptions in the continuity of its scanning trajectory and the integrity of spatial information. Enhancing the generalization ability and robustness of visual Mamba remains an unresolved challenge in the field.

VI. FUTURE DIRECTIONS

In this section, in order to advance the development of visual Mamba models, we outline several promising research directions that could potentially expand their capabilities and applications in computer vision.

A. Data

1) *Data Efficiency*: Given that Mamba exhibits a computational cost comparable to that of CNNs, it possesses significant potential to deliver optimal performance even without reliance on large-scale datasets. This attribute positions Mamba as a promising candidate for a variety of downstream tasks/multi-tasks and tasks involving the adaptation of pre-trained models.

2) *High-resolution Data*: Since the architecture of SSMs theoretically simplifies computation complexity, its potential for effectively handling high-resolution data, such as remote sensing and whole slice images, or long-term sequence data like long-term video frames holds considerable value.

3) *Multi-modal Data*: Just as the Transformer architecture has demonstrated its capability to model both natural languages and images within a unified framework, the Mamba model’s proficiency in handling extended sequences significantly broadens its applicability in multi-modal learning.

4) *In-context Learning*: In the dynamic landscape of deep learning, in-context learning has evolved to incorporate increasingly sophisticated and novel methodologies to address complex tasks across NLP, CV, and multi-modal domains. This methodological advancement is pivotal for pushing the limits of existing deep learning frameworks. The Mamba model, with its proficient in-context modeling capabilities and adeptness at capturing long-range dependencies, shows promising potential for deeper semantic understanding and enhanced performance in in-context learning applications.

B. Algorithm

1) *Scanning Techniques*: The selective scanning mechanism is a central component of the Mamba model, originally optimized for 1D causal sequential data. To address the inherently non-causal nature of visual data, many existing approaches employ bi-directional scanning. Additionally, to capture the spatial information inherent in 2D or higher-dimensional visual data, current approaches typically extend the scanning directions. Despite these adaptations, there is a pressing need for more innovative scanning schemes to harness the full potential of higher-dimensional non-causal visual data more effectively.

2) *Fusion Techniques*: Adapting the Mamba model to vision tasks often introduces redundancy, making the effective fusion of scanning output features an important area for further exploration. Additionally, foundational models in computer vision each possess unique strengths; for instance, CNNs inherently capture inductive biases like translation equivariance, while ViTs are noted for their robust modeling capabilities. Exploring methods to fuse features extracted by these diverse network architectures to maximize their advantages presents a valuable research opportunity.

3) *Computation Efficiency*: Mamba achieves linear scalability with respect to sequence length, but adapting it for vision tasks leads to increased computational demands due to the necessity of scanning in multiple paths. Consequently, there is a significant research opportunity in developing a more efficient and effective visual Mamba model. Furthermore, the Mamba model does not consistently outperform the Transformer in terms of computational efficiency, highlighting the need for optimized, hardware-aware Mamba algorithms tailored for visual tasks. This presents a promising avenue for research, particularly in developing approaches that reduce computational overhead while maintaining or enhancing performance. Enhancing the computational efficiency of visual Mamba models could greatly benefit their applicability in real-world scenarios.

VII. CONCLUSION

Mamba has rapidly emerged as a transformative long sequence modeling architecture, renowned for its exceptional

performance and efficient computational implementation. As it continues to gain significant traction in the field of computer vision, this paper offers a comprehensive review of visual Mamba approaches. We begin with an in-depth overview of the Mamba architecture, progressing to detailed examinations of representative visual Mamba backbone networks and their extensive applications across various visual domains. These applications are systematically categorized by differing modalities, including image, video, point cloud, and multi-modal data, among others. We conclude by critically analyzing the challenges associated with visual Mamba, highlighting the yet untapped potential of this architecture for advancing computer vision. Drawing on this analysis, we delineate future research directions for visual Mamba, providing valuable insights that may influence ongoing and future developments in this dynamically evolving field.

REFERENCES

- [1] A. Krizhevsky, I. Sutskever, and G. E. Hinton, "Imagenet classification with deep convolutional neural networks," in *NeurIPS*, 2012, pp. 1106–1114.
- [2] K. Simonyan and A. Zisserman, "Very deep convolutional networks for large-scale image recognition," in *ICLR*, 2015.
- [3] K. He, X. Zhang, S. Ren, and J. Sun, "Deep residual learning for image recognition," in *CVPR*, 2016, pp. 770–778.
- [4] A. Dosovitskiy, L. Beyer, A. Kolesnikov, D. Weissenborn, X. Zhai, T. Unterthiner, M. Dehghani, M. Minderer, G. Heigold, S. Gelly, J. Uszkoreit, and N. Houlsby, "An image is worth 16x16 words: Transformers for image recognition at scale," in *ICLR*, 2021.
- [5] A. Vaswani, N. Shazeer, N. Parmar, J. Uszkoreit, L. Jones, A. N. Gomez, L. Kaiser, and I. Polosukhin, "Attention is all you need," in *NeurIPS*, 2017, pp. 5998–6008.
- [6] Z. Liu, Y. Lin, Y. Cao, H. Hu, Y. Wei, Z. Zhang, S. Lin, and B. Guo, "Swin transformer: Hierarchical vision transformer using shifted windows," in *ICCV*. IEEE, 2021, pp. 9992–10002.
- [7] A. Gu, K. Goel, and C. Ré, "Efficiently modeling long sequences with structured state spaces," in *ICLR*, 2022.
- [8] A. Gu, I. Johnson, A. Timalina, A. Rudra, and C. Ré, "How to train your HIPPO: state space models with generalized orthogonal basis projections," in *ICLR*, 2023.
- [9] A. Gu, T. Dao, S. Ermon, A. Rudra, and C. Ré, "Hippo: Recurrent memory with optimal polynomial projections," in *NeurIPS*, 2020.
- [10] D. Hafner, T. P. Lillicrap, J. Ba, and M. Norouzi, "Dream to control: Learning behaviors by latent imagination," in *ICLR*, 2020.
- [11] K. J. Friston, L. M. Harrison, and W. D. Penny, "Dynamic causal modelling," *NeuroImage*, vol. 19, no. 4, pp. 1273–1302, 2003.
- [12] R. E. Kalman, "A New Approach to Linear Filtering and Prediction Problems," *Journal of Basic Engineering*, vol. 82, no. 1, pp. 35–45, 1960.
- [13] A. Gu, I. Johnson, K. Goel, K. Saab, T. Dao, A. Rudra, and C. Ré, "Combining recurrent, convolutional, and continuous-time models with linear state space layers," in *NeurIPS*, 2021, pp. 572–585.
- [14] A. Gu, K. Goel, A. Gupta, and C. Ré, "On the parameterization and initialization of diagonal state space models," in *NeurIPS*, 2022.
- [15] A. Gupta, A. Gu, and J. Berant, "Diagonal state spaces are as effective as structured state spaces," in *NeurIPS*, 2022.
- [16] A. Orvieto, S. L. Smith, A. Gu, A. Fernando, Ç. Gülçehre, R. Pascanu, and S. De, "Resurrecting recurrent neural networks for long sequences," in *ICML*, vol. 202, 2023, pp. 26 670–26 698.
- [17] J. T. H. Smith, A. Warrington, and S. W. Linderman, "Simplified state space layers for sequence modeling," in *ICLR*, 2023.
- [18] R. M. Hasani, M. Lechner, T. Wang, M. Chahine, A. Amini, and D. Rus, "Liquid structural state-space models," in *ICLR*, 2023.
- [19] A. Gu and T. Dao, "Mamba: Linear-time sequence modeling with selective state spaces," *arXiv preprint arXiv:2312.00752*, 2023.
- [20] Y. Liu, Y. Tian, Y. Zhao, H. Yu, L. Xie, Y. Wang, Q. Ye, and Y. Liu, "Vmamba: Visual state space model," *arXiv preprint arXiv:2401.10166*, 2024.
- [21] L. Zhu, B. Liao, Q. Zhang, X. Wang, W. Liu, and X. Wang, "Vision mamba: Efficient visual representation learning with bidirectional state space model," *arXiv preprint arXiv:2401.09417*, 2024.
- [22] S. Li, H. Singh, and A. Grover, "Mamba-nd: Selective state space modeling for multi-dimensional data," *arXiv preprint arXiv:2402.05892*, 2024.
- [23] C. Yang, Z. Chen, M. Espinosa, L. Ericsson, Z. Wang, J. Liu, and E. J. Crowley, "Plainmamba: Improving non-hierarchical mamba in visual recognition," *arXiv preprint arXiv:2403.17695*, 2024.
- [24] B. N. Patro and V. S. Agneeswaran, "Simba: Simplified mamba-based architecture for vision and multivariate time series," *arXiv preprint arXiv:2403.15360*, 2024.
- [25] T. Huang, X. Pei, S. You, F. Wang, C. Qian, and C. Xu, "Localmamba: Visual state space model with windowed selective scan," *arXiv preprint arXiv:2403.09338*, 2024.
- [26] X. Pei, T. Huang, and C. Xu, "Efficientvmamba: Atrous selective scan for light weight visual mamba," *arXiv preprint arXiv:2403.09977*, 2024.
- [27] A. Tustin, "A method of analysing the behaviour of linear systems in terms of time series," *Journal of the Institution of Electrical Engineers-Part IIA: Automatic Regulators and Servo Mechanisms*, vol. 94, no. 1, pp. 130–142, 1947.
- [28] D. Y. Fu, T. Dao, K. K. Saab, A. W. Thomas, A. Rudra, and C. Ré, "Hungry hungry hippos: Towards language modeling with state space models," in *ICLR*, 2023.
- [29] I. Radosavovic, R. P. Kosaraju, R. B. Girshick, K. He, and P. Dollár, "Designing network design spaces," in *CVPR*, 2020, pp. 10 425–10 433.
- [30] M. Tan and Q. V. Le, "Efficientnet: Rethinking model scaling for convolutional neural networks," in *ICML*, K. Chaudhuri and R. Salakhutdinov, Eds., vol. 97, 2019, pp. 6105–6114.
- [31] H. Touvron, M. Cord, M. Douze, F. Massa, A. Sablayrolles, and H. Jégou, "Training data-efficient image transformers & distillation through attention," in *ICML*, vol. 139, 2021, pp. 10 347–10 357.
- [32] E. Nguyen, K. Goel, A. Gu, G. W. Downs, P. Shah, T. Dao, S. Baccus, and C. Ré, "S4ND: modeling images and videos as multidimensional signals with state spaces," in *NeurIPS*, 2022.
- [33] K. He, G. Kioxari, P. Dollár, and R. B. Girshick, "Mask R-CNN," in *ICCV*, 2017, pp. 2980–2988.
- [34] S. Xie, R. B. Girshick, P. Dollár, Z. Tu, and K. He, "Aggregated residual transformations for deep neural networks," in *CVPR*, 2017, pp. 5987–5995.
- [35] Z. Liu, H. Mao, C. Wu, C. Feichtenhofer, T. Darrell, and S. Xie, "A convnet for the 2020s," in *CVPR*, 2022, pp. 11 966–11 976.
- [36] Z. Chen, Y. Duan, W. Wang, J. He, T. Lu, J. Dai, and Y. Qiao, "Vision transformer adapter for dense predictions," in *ICLR*, 2023.
- [37] W. Wang, E. Xie, X. Li, D. Fan, K. Song, D. Liang, T. Lu, P. Luo, and L. Shao, "Pyramid vision transformer: A versatile backbone for dense prediction without convolutions," in *ICCV*, 2021, pp. 548–558.
- [38] P. Zhang, X. Dai, J. Yang, B. Xiao, L. Yuan, L. Zhang, and J. Gao, "Multi-scale vision longformer: A new vision transformer for high-resolution image encoding," in *iccv21/vil*, 2021, pp. 2978–2988.
- [39] T. Xiao, Y. Liu, B. Zhou, Y. Jiang, and J. Sun, "Unified perceptual parsing for scene understanding," in *ECCV*, vol. 11209. Springer, 2018, pp. 432–448.
- [40] H. Touvron, M. Cord, and H. Jégou, "Deit III: revenge of the vit," in *ECCV*, vol. 13684. Springer, 2022, pp. 516–533.
- [41] J. Devlin, M. Chang, K. Lee, and K. Toutanova, "BERT: pre-training of deep bidirectional transformers for language understanding," in *NAACL-HLT*, 2019, pp. 4171–4186.
- [42] Z. Liu, H. Hu, Y. Lin, Z. Yao, Z. Xie, Y. Wei, J. Ning, Y. Cao, Z. Zhang, L. Dong, F. Wei, and B. Guo, "Swin transformer V2: scaling up capacity and resolution," in *CVPR*, 2022, pp. 11 999–12 009.
- [43] J. Deng, W. Dong, R. Socher, L. Li, K. Li, and L. Fei-Fei, "Imagenet: A large-scale hierarchical image database," in *CVPR*, 2009, pp. 248–255.
- [44] T. Lin, M. Maire, S. J. Belongie, J. Hays, P. Perona, D. Ramanan, P. Dollár, and C. L. Zitnick, "Microsoft COCO: common objects in context," in *ECCV*, ser. Lecture Notes in Computer Science, vol. 8693. Springer, 2014, pp. 740–755.
- [45] B. Zhou, H. Zhao, X. Puig, T. Xiao, S. Fidler, A. Barriuso, and A. Torralba, "Semantic understanding of scenes through the ADE20K dataset," *Int. J. Comput. Vis.*, vol. 127, no. 3, pp. 302–321, 2019.
- [46] Y. Yue and Z. Li, "Medmamba: Vision mamba for medical image classification," *arXiv preprint arXiv:2403.03849*, 2024.
- [47] Z. Fang, Y. Wang, Z. Wang, J. Zhang, X. Ji, and Y. Zhang, "Mammil: Multiple instance learning for whole slide images with state space models," *arXiv preprint arXiv:2403.05160*, 2024.
- [48] S. Yang, Y. Wang, and H. Chen, "Mambamil: Enhancing long sequence modeling with sequence reordering in computational pathology," *arXiv preprint arXiv:2403.06800*, 2024.

- [49] G. Yang, K. Du, Z. Yang, Y. Du, Y. Zheng, and S. Wang, "Cmvim: Contrastive masked vim autoencoder for 3d multi-modal representation learning for ad classification," *arXiv preprint arXiv:2403.16520*, 2024.
- [50] K. Chen, B. Chen, C. Liu, W. Li, Z. Zou, and Z. Shi, "Rsmamba: Remote sensing image classification with state space model," *arXiv preprint arXiv:2403.19654*, 2024.
- [51] J. Ma, F. Li, and B. Wang, "U-mamba: Enhancing long-range dependency for biomedical image segmentation," *arXiv preprint arXiv:2401.04722*, 2024.
- [52] Z. Xing, T. Ye, Y. Yang, G. Liu, and L. Zhu, "Segmamba: Long-range sequential modeling mamba for 3d medical image segmentation," *arXiv preprint arXiv:2401.13560*, 2024.
- [53] J. Ruan and S. Xiang, "Vm-UNET: Vision mamba unet for medical image segmentation," *arXiv preprint arXiv:2402.02491*, 2024.
- [54] J. Liu, H. Yang, H.-Y. Zhou, Y. Xi, L. Yu, Y. Yu, Y. Liang, G. Shi, S. Zhang, H. Zheng *et al.*, "Swin-umamba: Mamba-based unet with imagenet-based pretraining," *arXiv preprint arXiv:2402.03302*, 2024.
- [55] Z. Wang, J.-Q. Zheng, Y. Zhang, G. Cui, and L. Li, "Mamba-unet: Unet-like pure visual mamba for medical image segmentation," *arXiv preprint arXiv:2402.05079*, 2024.
- [56] C. Ma and Z. Wang, "Semi-mamba-unet: Pixel-level contrastive and pixel-level cross-supervised visual mamba-based unet for semi-supervised medical image segmentation," *arXiv e-prints*, pp. arXiv-2402, 2024.
- [57] Z. Ye and T. Chen, "P-mamba: Marrying perona malik diffusion with mamba for efficient pediatric echocardiographic left ventricular segmentation," *arXiv preprint arXiv:2402.08506*, 2024.
- [58] Z. Wang and C. Ma, "Weak-mamba-unet: Visual mamba makes cnn and vit work better for scribble-based medical image segmentation," *arXiv preprint arXiv:2402.10887*, 2024.
- [59] T. Chen, Z. Tan, T. Gong, Q. Chu, Y. Wu, B. Liu, J. Ye, and N. Yu, "Mim-istd: Mamba-in-mamba for efficient infrared small target detection," *arXiv preprint arXiv:2403.02148*, 2024.
- [60] W. Liao, Y. Zhu, X. Wang, C. Pan, Y. Wang, and L. Ma, "Lightm-unet: Mamba assists in lightweight unet for medical image segmentation," *arXiv preprint arXiv:2403.05246*, 2024.
- [61] J. Wang, J. Chen, D. Chen, and J. Wu, "Large window-based mamba unet for medical image segmentation: Beyond convolution and self-attention," *arXiv preprint arXiv:2403.07332*, 2024.
- [62] M. Zhang, Y. Yu, L. Gu, T. Lin, and X. Tao, "Vm-unet-v2 rethinking vision mamba unet for medical image segmentation," *arXiv preprint arXiv:2403.09157*, 2024.
- [63] R. Wu, Y. Liu, P. Liang, and Q. Chang, "H-vmunet: High-order vision mamba unet for medical image segmentation," *arXiv preprint arXiv:2403.13642*, 2024.
- [64] J. Xie, R. Liao, Z. Zhang, S. Yi, Y. Zhu, and G. Luo, "Promamba: Prompt-mamba for polyp segmentation," *arXiv preprint arXiv:2403.13660*, 2024.
- [65] H. Tang, L. Cheng, G. Huang, Z. Tan, J. Lu, and K. Wu, "Rotate to scan: Unet-like mamba with triplet ssm module for medical image segmentation," *arXiv preprint arXiv:2403.17701*, 2024.
- [66] K. S. Sanjid, M. T. Hossain, M. S. S. Junayed, and D. M. M. Uddin, "Integrating mamba sequence model and hierarchical upsampling network for accurate semantic segmentation of multiple sclerosis legion," *arXiv preprint arXiv:2403.17432*, 2024.
- [67] R. Wu, Y. Liu, P. Liang, and Q. Chang, "Ultralight vm-unet: Parallel vision mamba significantly reduces parameters for skin lesion segmentation," *arXiv preprint arXiv:2403.20035*, 2024.
- [68] J. Hao, L. He, and K. F. Hung, "T-mamba: Frequency-enhanced gated long-range dependency for tooth 3d cbct segmentation," *arXiv preprint arXiv:2404.01065*, 2024.
- [69] Q. Zhu, Y. Cai, Y. Fang, Y. Yang, C. Chen, L. Fan, and A. Nguyen, "Samba: Semantic segmentation of remotely sensed images with state space model," *arXiv preprint arXiv:2404.01705*, 2024.
- [70] X. Ma, X. Zhang, and M.-O. Pun, "Rs3mamba: Visual state space model for remote sensing images semantic segmentation," *arXiv preprint arXiv:2404.02457*, 2024.
- [71] S. Zhao, H. Chen, X. Zhang, P. Xiao, L. Bai, and W. Ouyang, "Rs-mamba for large remote sensing image dense prediction," *arXiv preprint arXiv:2404.02668*, 2024.
- [72] H. Chen, J. Song, C. Han, J. Xia, and N. Yokoya, "Changemamba: Remote sensing change detection with spatio-temporal state space model," *arXiv preprint arXiv:2404.03425*, 2024.
- [73] L. Fu, X. Li, X. Cai, Y. Wang, X. Wang, Y. Shen, and Y. Yao, "Md-dose: A diffusion model based on the mamba for radiotherapy dose prediction," *arXiv preprint arXiv:2403.08479*, 2024.
- [74] V. T. Hu, S. A. Baumann, M. Gui, O. Grebenkova, P. Ma, J. Fischer, and B. Ommer, "Zigma: Zigzag mamba diffusion model," *arXiv preprint arXiv:2403.13802*, 2024.
- [75] Q. Shen, X. Yi, Z. Wu, P. Zhou, H. Zhang, S. Yan, and X. Wang, "Gamba: Marry gaussian splatting with mamba for single view 3d reconstruction," *arXiv preprint arXiv:2403.18795*, 2024.
- [76] Z. Zheng and C. Wu, "U-shaped vision mamba for single image dehazing," *arXiv preprint arXiv:2402.04139*, 2024.
- [77] Z. Zheng and J. Zhang, "Fd-vision mamba for endoscopic exposure correction," *arXiv preprint arXiv:2402.06378*, 2024.
- [78] X. He, K. Cao, K. Yan, R. Li, C. Xie, J. Zhang, and M. Zhou, "Pan-mamba: Effective pan-sharpening with state space model," *arXiv preprint arXiv:2402.12192*, 2024.
- [79] H. Guo, J. Li, T. Dai, Z. Ouyang, X. Ren, and S.-T. Xia, "Mambair: A simple baseline for image restoration with state-space model," *arXiv preprint arXiv:2402.15648*, 2024.
- [80] J. Huang, L. Yang, F. Wang, Y. Wu, Y. Nan, A. I. Aviles-Rivero, C.-B. Schönlieb, D. Zhang, and G. Yang, "Mambamir: An arbitrary-masked mamba for joint medical image reconstruction and uncertainty estimation," *arXiv preprint arXiv:2402.18451*, 2024.
- [81] C. Cheng, H. Wang, and H. Sun, "Activating wider areas in image super-resolution," *arXiv preprint arXiv:2403.08330*, 2024.
- [82] Z. Chen and Y. Ge, "Mambauie: Unraveling the ocean's secrets with only 2.8 flops," *arXiv preprint arXiv:2404.13884*, 2024.
- [83] Z. Shao, H. Bian, Y. Chen, Y. Wang, J. Zhang, X. Ji *et al.*, "Transmil: Transformer based correlated multiple instance learning for whole slide image classification," *Advances in neural information processing systems*, vol. 34, pp. 2136–2147, 2021.
- [84] Y. Yang, Z. Xing, C. Huang, and L. Zhu, "Vivim: a video vision mamba for medical video object segmentation," *arXiv preprint arXiv:2401.14168*, 2024.
- [85] K. Li, X. Li, Y. Wang, Y. He, Y. Wang, L. Wang, and Y. Qiao, "Videomamba: State space model for efficient video understanding," *arXiv preprint arXiv:2403.06977*, 2024.
- [86] G. Chen, Y. Huang, J. Xu, B. Pei, Z. Chen, Z. Li, J. Wang, K. Li, T. Lu, and L. Wang, "Video mamba suite: State space model as a versatile alternative for video understanding," *arXiv preprint arXiv:2403.09626*, 2024.
- [87] B. Zou, Z. Guo, X. Hu, and H. Ma, "Rhythmmamba: Fast remote physiological measurement with arbitrary length videos," *arXiv preprint arXiv:2404.06483*, 2024.
- [88] S. Chaudhuri and S. Bhattacharya, "Simba: Mamba augmented u-shiftgcn for skeletal action recognition in videos," *arXiv preprint arXiv:2404.07645*, 2024.
- [89] T. Guo, Y. Wang, S. Shu, D. Chen, Z. Tang, C. Meng, and X. Bai, "Mambamorph: a mamba-based framework for medical mr-ct deformable registration," *arXiv preprint arXiv:2401.13934*, 2024.
- [90] Z. Zhang, A. Liu, I. Reid, R. Hartley, B. Zhuang, and H. Tang, "Motion mamba: Efficient and long sequence motion generation with hierarchical and bidirectional selective ssm," *arXiv preprint arXiv:2403.07487*, 2024.
- [91] Y. Qiao, Z. Yu, L. Guo, S. Chen, Z. Zhao, M. Sun, Q. Wu, and J. Liu, "Vl-mamba: Exploring state space models for multimodal learning," *arXiv preprint arXiv:2403.13600*, 2024.
- [92] H. Zhao, M. Zhang, W. Zhao, P. Ding, S. Huang, and D. Wang, "Cobra: Extending mamba to multi-modal large language model for efficient inference," *arXiv preprint arXiv:2403.14520*, 2024.
- [93] Y. Yang, C. Ma, J. Yao, Z. Zhong, Y. Zhang, and Y. Wang, "Remember: Referring image segmentation with mamba twister," *arXiv preprint arXiv:2403.17839*, 2024.
- [94] W. Li, X. Hong, and X. Fan, "Spikemba: Multi-modal spiking saliency mamba for temporal video grounding," *arXiv preprint arXiv:2404.01174*, 2024.
- [95] Z. Wan, Y. Wang, S. Yong, P. Zhang, S. Stepputtis, K. Sycara, and Y. Xie, "Sigma: Siamese mamba network for multi-modal semantic segmentation," *arXiv preprint arXiv:2404.04256*, 2024.
- [96] Y. Chen, J. Xie, Y. Lin, Y. Song, W. Yang, and R. Yu, "SurvMamba: State space model with multi-grained multi-modal interaction for survival prediction," *arXiv preprint arXiv:2404.08027*, 2024.
- [97] S. Peng, X. Zhu, H. Deng, Z. Lei, and L.-J. Deng, "Fusion-mamba: Efficient image fusion with state space model," *arXiv preprint arXiv:2404.07932*, 2024.
- [98] Z. Li, H. Pan, K. Zhang, Y. Wang, and F. Yu, "Mambadfuse: A mamba-based dual-phase model for multi-modality image fusion," *arXiv preprint arXiv:2404.08406*, 2024.

- [99] W. Dong, H. Zhu, S. Lin, X. Luo, Y. Shen, X. Liu, J. Zhang, G. Guo, and B. Zhang, "Fusion-mamba for cross-modality object detection," *arXiv preprint arXiv:2404.09146*, 2024.
- [100] X. Xie, Y. Cui, C.-I. Jeong, T. Tan, X. Zhang, X. Zheng, and Z. Yu, "Fusionmamba: Dynamic feature enhancement for multimodal image fusion with mamba," *arXiv preprint arXiv:2404.09498*, 2024.
- [101] X. Wang, Z. Kang, and Y. Mu, "Text-controlled motion mamba: Text-instructed temporal grounding of human motion," *arXiv preprint arXiv:2404.11375*, 2024.
- [102] D. Liang, X. Zhou, X. Wang, X. Zhu, W. Xu, Z. Zou, X. Ye, and X. Bai, "Pointmamba: A simple state space model for point cloud analysis," *arXiv preprint arXiv:2402.10739*, 2024.
- [103] T. Zhang, X. Li, H. Yuan, S. Ji, and S. Yan, "Point could mamba: Point cloud learning via state space model," *arXiv preprint arXiv:2403.00762*, 2024.
- [104] J. Liu, R. Yu, Y. Wang, Y. Zheng, T. Deng, W. Ye, and H. Wang, "Point mamba: A novel point cloud backbone based on state space model with octree-based ordering strategy," *arXiv preprint arXiv:2403.06467*, 2024.
- [105] Q. Zhou, W. Yang, B. Fei, J. Xu, R. Zhang, K. Liu, Y. Luo, and Y. He, "3dmambaipf: A state space model for iterative point cloud filtering via differentiable rendering," *arXiv preprint arXiv:2404.05522*, 2024.
- [106] Y. Li, W. Yang, and B. Fei, "3dmambacomplete: Exploring structured state space model for point cloud completion," *arXiv preprint arXiv:2404.07106*, 2024.
- [107] X. Han, Y. Tang, Z. Wang, and X. Li, "Mamba3d: Enhancing local features for 3d point cloud analysis via state space model," *arXiv preprint arXiv:2404.14966*, 2024.
- [108] H. Touvron, T. Lavril, G. Izacard, X. Martinet, M.-A. Lachaux, T. Lacroix, B. Rozière, N. Goyal, E. Hambro, F. Azhar *et al.*, "Llama: Open and efficient foundation language models," *arXiv preprint arXiv:2302.13971*, 2023.
- [109] M. Oquab, T. Darcet, T. Moutakanni, H. Vo, M. Szafraniec, V. Khalidov, P. Fernandez, D. Haziza, F. Massa, A. El-Nouby *et al.*, "Dinov2: Learning robust visual features without supervision," *arXiv preprint arXiv:2304.07193*, 2023.
- [110] X. Zhai, B. Mustafa, A. Kolesnikov, and L. Beyer, "Sigmoid loss for language image pre-training," in *Proceedings of the IEEE/CVF International Conference on Computer Vision*, 2023, pp. 11 975–11 986.
- [111] X. Wang, S. Wang, Y. Ding, Y. Li, W. Wu, Y. Rong, W. Kong, J. Huang, S. Li, H. Yang, Z. Wang, B. Jiang, C. Li, Y. Wang, Y. Tian, and J. Tang, "State space model for new-generation network alternative to transformers: A survey," *arXiv preprint arXiv:2404.09516*, 2024.
- [112] R. Grazzi, J. Siems, S. Schrodli, T. Brox, and F. Hutter, "Is mamba capable of in-context learning?" *arXiv preprint arXiv:2402.03170*, 2024.
- [113] J. Park, J. Park, Z. Xiong, N. Lee, J. Cho, S. Oymak, K. Lee, and D. Papailiopoulos, "Can mamba learn how to learn? A comparative study on in-context learning tasks," *arXiv preprint arXiv:2402.04248*, 2024.
- [114] A. S. Sharma, D. Atkinson, and D. Bau, "Locating and editing factual associations in mamba," *arXiv preprint arXiv:2404.03646*, 2024.
- [115] N. M. Cirone, A. Orvieto, B. Walker, C. Salvi, and T. J. Lyons, "Theoretical foundations of deep selective state-space models," *arXiv preprint arXiv:2402.19047*, 2024.
- [116] A. Ali, I. Zimmerman, and L. Wolf, "The hidden attention of mamba models," *arXiv preprint arXiv:2403.01590*, 2024.
- [117] S. Long, Q. Zhou, X. Li, X. Lu, C. Ying, Y. Luo, L. Ma, and S. Yan, "Dgmamba: Domain generalization via generalized state space model," *arXiv preprint arXiv:2404.07794*, 2024.
- [118] C. Du, Y. Li, and C. Xu, "Understanding robustness of visual state space models for image classification," *arXiv preprint arXiv:2403.10935*, 2024.